Chapter 5

Lewis Acid-Assisted CO_2 Reduction

Chapter 5

Introduction

Combustion of fossil fuels generates some of the vast abundance of atmospheric CO_2; carbon neutrality could be achieved by recycling the produced CO_2 through catalytic conversion to fuels and chemicals.[1] The two main approaches to CO_2 reduction are electrocatalysis,[1a] in which protons and electrons are sequentially (and/or concertedly) added, and hydrogenation,[1b] in which H_2 is the source of protons and electrons (Scheme 5.1). While in principle the products could be the same, most of the electrocatalytic systems generate CO and H_2O (at quite reducing potentials), while the hydrogenation systems generally produce formic acid (under forcing pressures), as depicted in Scheme 5.1. Lewis and Brønsted acid additives, particularly from the alkali and alkaline earth metals, have shown promise in improving electrocatalytic CO_2 reduction, notably in low-valent Fe porphyrins.[2] Bimetallic catalysts, including biological [NiFe] CO dehydrogenase, feature one metal bound to C while another metal binds O, acting as a Lewis acid.[3] Similar Lewis acid (e.g., AlO_x, TiO_x) enhancements have been noted in heterogeneous systems that convert CO_2 and CO to CH_4.[4] Stoichiometric boron additives in homogeneous Cu[5] and Ni[6] systems have also been reported, wherein a diborane B–B[5] or secondary borane B–H[6] bond is replaced with a B–O bond to help drive a reaction. These homogeneous catalytic reactions effectively replace H_2 with borane reductants. "Frustrated Lewis pairs"[7] have also utilized the strength of B–O bonds to stabilize reduced CO_2 products, including methanol

upon hydrolysis.[8] Catalytic B–O bond cleavage in all of these cases is difficult, if not impossible; presently, stoichiometric boranes are required.

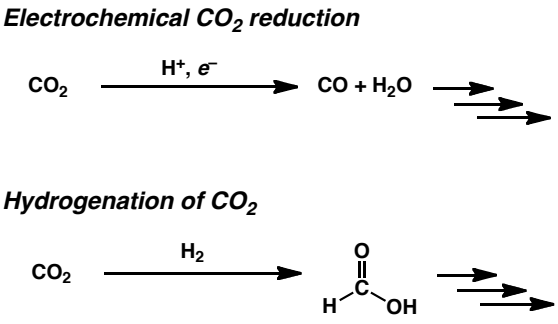

Scheme 5.1

Chemical industry generates concentrated CO_2 streams as a flue gas, the utilization of which would be convenient relative to collection of CO_2 dispersed in the atmosphere. CO_2 is also an impurity in key pipeline feedstocks such as synthesis gas (CO + H_2). An ideal syngas conversion catalyst would either be tolerant to CO_2, or would react equally well with CO_2 to form reduced products. The widely implemented $CuO/ZnO/Al_2O_3$ catalyst that converts syngas to methanol meets this requirement, converting a mixture of CO_2 and CO to methanol.[9] Our interest in syngas conversion to higher organics[10] initially prompted us to examine the reactivity of CO_2 with partially reduced M–CO species and the late transition metal hydride species employed in CO reduction. Further, a CO_2-tolerant catalyst could hypothetically utilize the CO produced by electrocatalytic CO_2 reduction to generate further reduced products.

We report here that the late transition metal hydrides and reduced metal carbonyl components of our CO reductive coupling system both reduce CO_2 to $[HCO_2]^-$. The

Lewis acidic trialkylboranes — which promote CO reductive coupling — also play a key role in facilitating CO_2 reduction. The resulting formate-borane adduct is quite weakly bound relative to the strong covalent bonds to boron discussed above, signifying a promising new approach to promoting CO_2 reduction by H_2 with Ni/BR_3 cooperation.

Results and Discussion

Reactivity of rhenium species with CO_2.

We have previously reported that the Re carbonyl cation $[(Ph_2P(CH_2)_2B(C_8H_{14})_2Re(CO)_4][BF_4]$ ([**1**][BF_4]), bearing pendent alkylboranes in the secondary coordination sphere of the metal, is readily reduced by $NaHBEt_3$ or $[HPt(dmpe)_2][PF_6]$, initially forming boroxycarbene **2** before a second reduction initiates C–C coupling (Scheme 5.2).[10a] Further studies of **2** showed that it reacts as a relatively potent hydride source, releasing H_2 upon treatment with water or weak acids (Chapter 3).[10d]

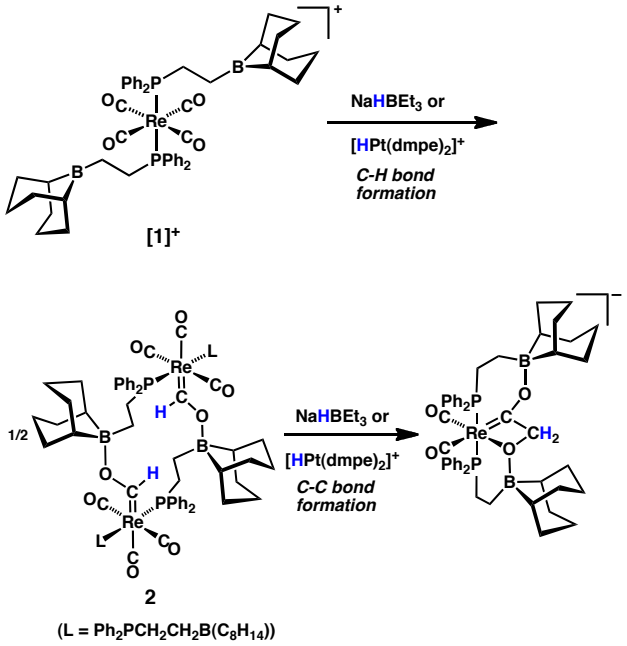

Scheme 5.2

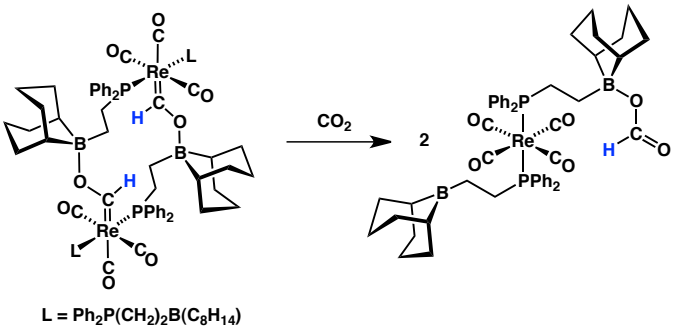

Scheme 5.3

A solution of **2**, formed *in situ* from [**1**][BF_4] and $NaHBEt_3$ in C_6D_5Cl,[10a] was degassed by three freeze—pump—thaw cycles before admission of 1 atm CO_2. A few minutes later a new ^1H NMR resonance was observed at δ 8.44. ^{31}P NMR showed complete consumption of **2** and formation of a symmetric Re product with a chemical shift similar to [**1**]$^+$. Infrared spectroscopy confirmed the presence of a $Re(CO)_4^+$ core (single strong stretch at 1993 cm^{-1}) and a C=O functionality (1620 cm^{-1}). The spectroscopic data point to hydride transfer

from **2** to CO_2 to form [**1**]$^+$ and $[HCO_2]^-$, which form an adduct, **1**•(HCO_2) (Scheme 5.3). The NMR spectra are consistent with a high symmetry species, presumably through fluxional processes such as exchange of formate between boranes or additional adduct formation.

After about an hour, large amounts of precipitate formed, and the signals corresponding to **1**•(HCO_2) dissipated; we speculate that this is due to oligomerization of **1**•(HCO_2) through the two oxygens of formate (i.e., R_3B–OC(H)O–BR_3). Similar oligomerization was observed for the series $(Ph_2P(CH_2)_nB(C_8H_{14}))_2Re(CO)_3(CHO)$ (n = 2, 3): **2** (n = 2) undergoes monomer-dimer equilibrium in solution but crystallizes spontaneously from CH_2Cl_2 as a dimer;[10a] for n = 3, intermolecular B–O interactions appear to dominate, and the higher aggregates precipitate from solution.[10d] The presence of formate in **1**•(HCO_2) was further confirmed by addition of $[Bu_4N][HCO_2]$ to [**1**][BF_4] in C_6D_5Cl, which gave **1**•(HCO_2) as judged by ^{1}H, ^{31}P{^{1}H} NMR, and IR spectroscopy. **1**•(HCO_2) produced in this fashion also precipitated from C_6D_5Cl over the course of a few hours.

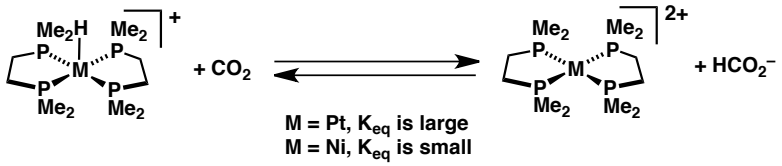

Scheme 5.4

We have used the platinum hydride $[HPt(dmpe)_2][PF_6]$, originally reported by DuBois,[11] extensively in CO reduction chemistry.[10a-d] This reagent is not compatible with CO_2: DuBois reported that $[HPt(dmpe)_2][PF_6]$ (ΔG_{H^-} = 42.5 kcal mol^{-1}) reduces CO_2 to HCO_2^- according to the equilibrium in Scheme 5.4. The hydride donor strength, ΔG_{H^-}, is known

for a large number of late transition metal bis(diphosphine) complexes;[12] smaller values indicate more facile dissociation of H^- and therefore more potent reductants. DuBois estimated that $[HCO_2]^-$ is a hydride donor of similar potency to $[HPt(depe)_2]^+$, ΔG_{H^-} = 44.2 kcal mol^{-1} (recalculated from the originally published value[12a] using DuBois' more recent pKa value[12d]). Weaker hydride donors, such as $[HNi(dmpe)_2][PF_6]$ (ΔG_{H^-} = 50.9 kcal mol^{-1}), do not reduce CO_2;[13] in fact the reverse reaction is observed, as $[Bu_4N][HCO_2]$ transfers hydride to $[Ni(dmpe)_2]^{2+}$ to yield $[HNi(dmpe)_2]^+$ (Scheme 5.4). Boroxycarbene **2** is intermediate in hydride strength between $[HNi(dmpe)_2][PF_6]$ and $[HPt(dmpe)_2][PF_6]$; it is readily formed from $[\mathbf{1}][BF_4]$ and $[HPt(dmpe)_2][PF_6]$, but mixtures of $[\mathbf{1}][BF_4]$ and $[HNi(dmpe)_2][PF_6]$ show no discernible reaction.

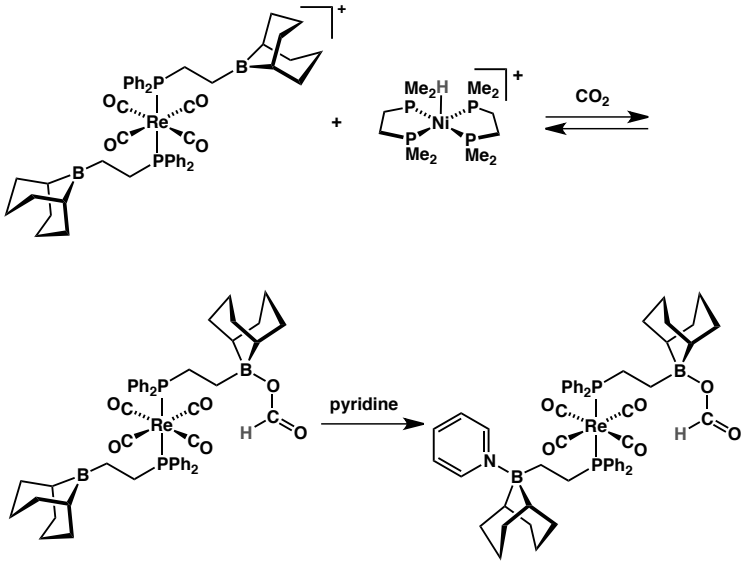

Scheme 5.5

Given the above observations, we were surprised to find that addition of CO_2 to a mixture of $[HNi(dmpe)_2][PF_6]$ and $[\mathbf{1}][BF_4]$ produced significant amounts of formate (δ 8.43) over 24 hours at room temperature (Scheme 5.5). The reaction did not proceed to completion,

as evidenced by the presence of unreacted $[HNi(dmpe)_2]^+$ and chemical shifts for the sole visible Re-containing species being intermediate between $[\mathbf{1}]^+$ and **1**•(HCO_2) (suggesting an equilibrium between these species). As in the reaction of **2** with CO_2, precipitates formed over time; boroxycarbene **2** was not observed before precipitation. The isolated precipitates partially dissolved upon treatment with pyridine, and signals from both the formate (δ 8.88) and phosphinoborane ligands (now in an asymmetric environment) were present (^{31}P NMR δ 1.95 d, 2.98 d, $\mathcal{J}_{PP}$ = 77 Hz). This species is assigned to zwittterionic **1**•$(HCO_2)(C_5H_5N)$, with one borane bound by pyridine and the other by formate; pyridine adduct formation would prevent oligomerization by binding the boranes to give soluble monomers.

Reactivity of group 9 and 10 hydrides with CO_2

Based on thermodynamic hydride donor strength, it is surprising that mixtures of $[HNi(dmpe)_2]^+$ and $[\mathbf{1}]^+$ reduce CO_2: the ultimate reaction is a transfer of hydride from $[HNi(dmpe)_2]^+$ to CO_2, which is apparently uphill by ~7 kcal mol^{-1} (Scheme 5.4).[13] Suspecting the central involvement of the Lewis acidic functionality of $[\mathbf{1}]^+$, $[HNi(dmpe)_2][PF_6]$ was allowed to react with 1 atm CO_2 in the presence of trialkylborane ^{t}Bu$(CH_2)_2$B(C_8H_{14}) in C_6D_5Cl (Scheme 5.7). Over a few hours, a ^{1}H NMR resonance at δ 8.73 grew in as the hydride resonance of $[HNi(dmpe)_2]^+$ diminished and $[Ni(dmpe)_2]^{2+}$ precipitated. The reaction did not go to completion, but NMR yields (~50% formate) were greatly increased relative to acid-free conditions (~5% formate). As the reaction proceeded, ^{1}H NMR resonances for formate shifted upfield ($[HCO_2]^-$ δ 8.73 at 2 h, 8.66 at 18 h) while the *tert*-butyl group of ^{t}Bu$(CH_2)_2$B(C_8H_{14}) shifted downfield (^{t}*Bu*$(CH_2)_2$B(C_8H_{14}), δ 0.89

initially, 0.95 at 2 h, 0.97 at 18 h). Monitoring the reaction by ^{11}B NMR spectroscopy showed significant peak broadening along with an upfield shift as the reaction proceeded (Figure 5.1; δ 88.2 initially, 65 at 2 h, 51 at 18 h).

The CO_2 reduction product is conclusively assigned to formate based on separate experiments adding authentic sources of formate and reducing $^{13}CO_2$ (*vide infra*). As in **1**•(HCO_2), the [*H*CO_2]$^-$ ^{1}H NMR resonance does not match that of "free" [Bu_4N][HCO_2]. The dynamic spectral shifts and broadening are ascribed to adduct formation between formate and the trialkylborane;[10c] addition of ^{t}Bu(CH_2)$_2$B(C_8H_{14}) to [Bu_4N][HCO_2] in C_6D_5Cl prompted an upfield shift in the *H*CO_2 ^{1}H NMR resonance from δ 9.58 (no borane) to δ 8.89 (one equivalent of borane). The latter value compares well to the reaction of [HNi(dmpe)$_2$][PF_6] with ^{t}Bu(CH_2)$_2$B(C_8H_{14}) and CO_2 after addition of hept$_4$NBr (δ 8.79).

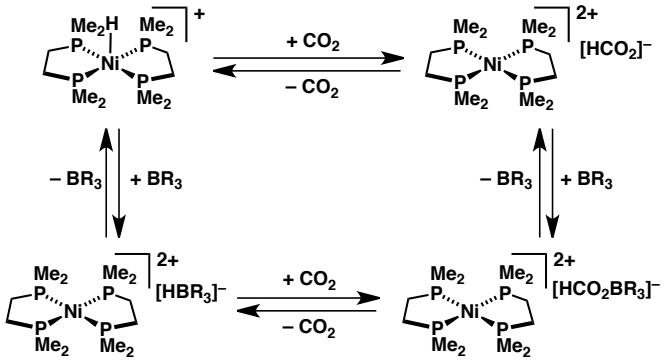

Scheme 5.6

The presence of a borane-formate adduct is also likely responsible for the enhanced CO_2 reduction chemistry of [HNi(dmpe)$_2$]$^+$. The mechanism of acid promotion (Scheme 5.6) could be thermodynamic in nature, if formate is stabilized by adduct formation by more

than 7 kcal mol^{-1} (the amount by which the reaction without borane is uphill, *vide supra*). The borane could play a kinetic role as well, such as through a "hydride shuttle" mechanism,[10d] but kinetic studies have not been undertaken as of yet. The reversible binding process exhibited by the borane-formate adduct could be extremely beneficial in a catalytic process, as compared to irreversible B–O formation in other catalytic transformations.

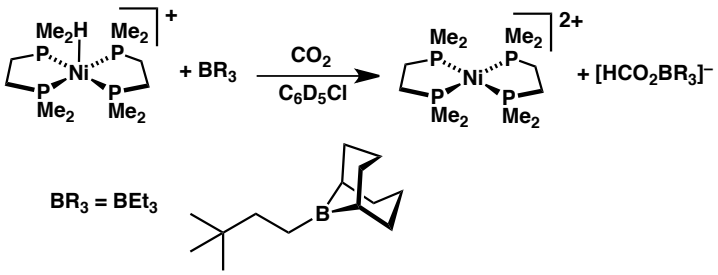

Scheme 5.7

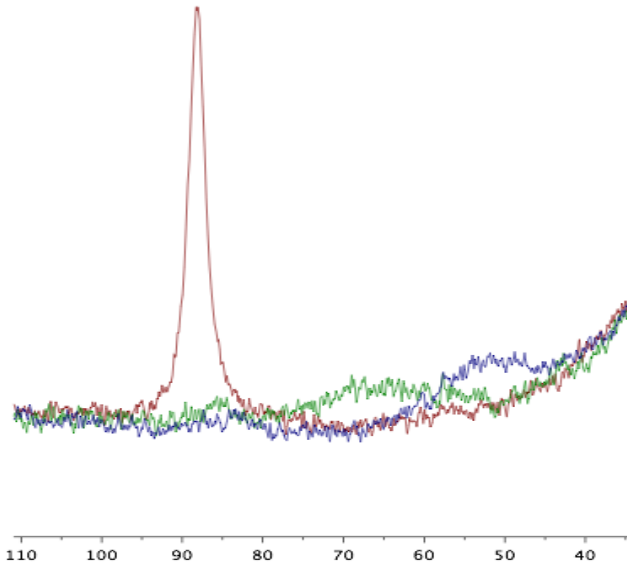

Figure 5.1. ^{11}B NMR spectra before CO_2 addition (red), after 2 hours (green), and after 18 hours (blue).

The reaction may stop at 50% conversion because of a natural equilibrium, or because of complications relating to precipitation of $[Ni(dmpe)_2]^{2+}$ from C_6D_5Cl. The slight shifts of the hydride signal of $[HNi(dmpe)_2]^+$ over the course of the reaction could be indicative of a change in counterion. Perhaps $[HNi(dmpe)_2][HCO_2]$ is stable relative to other species. The reaction was driven to completion upon addition of $hept_4NBr$ (and readmission of 1 atm CO_2). The tetraheptylammonium salt coaxes precipitation of $[Ni(dmpe)_2][Br]_2$ and provides a counter cation for $[HCO_2]^-$ other than either of the Ni species.

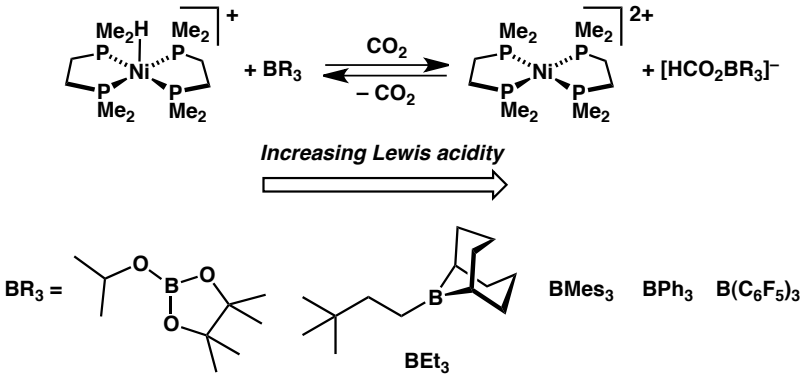

Scheme 5.8

A variety of boranes of varying Lewis acidity were employed in the reaction to assess the limits of Lewis acid assistance (Scheme 5.8). Isopropyl pinacol borate did not have any noticeable effect on the amount of formate produced. The small amount of formate that was produced resonated upfield of the formate produced in the absence of any Lewis acid (δ 8.84 vs. 8.74). Trimesitylborane also did not effect significant CO_2 reduction, perhaps due to steric constraints, but had a more pronounced upfield shift in the small amount of formate generated (δ 8.63), quite similar to the chemical shift in the trialkylborane

reactions. The upfield chemical shifts are consistent with some adduct formation, but the adduct appears to be disfavored by the less acidic and more bulky Lewis acids.

Addition of triphenylborane did impact the reduction, however: NMR monitoring showed formation of formate, along with some side products. The strong acid $B(C_6F_5)_3$ was also screened, but hydride transfer from Ni to B was observed before any CO_2 reduction could occur. A "frustrated Lewis pair" consisting of TMP (TMP = 2,2,6,6-tetramethylpiperidine) and $B(C_6F_5)_3$ have recently been shown to cleave H_2 to generate $[TMPH][HB(C_6F_5)_3]$, which reduces CO_2 to $HCO_2B(C_6F_5)_3$ at 100 °C.[8] We did not pursue this chemistry further, as we wished to avoid the strong B–O bonds of $HCO_2B(C_6F_5)_3$ and focus on Ni-based reactivity.

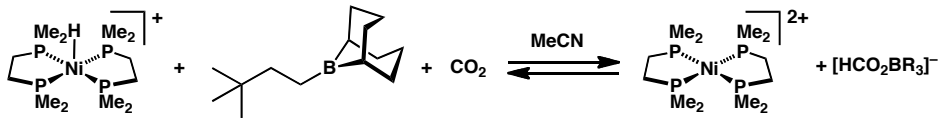

Scheme 5.9

All of the constituents are soluble in MeCN, which could allow observation of a true equilibrium process. Despite fears that MeCN would bind the borane too tightly to observe any acid assistance, treatment of $[HNi(dmpe)_2][PF_6]$ with 0-10 equiv $^tBu(CH_2)_2B(C_8H_{14})$ in CD_3CN did exhibit equilibrium behavior. With no added borane, ~5% conversion to $[Ni(dmpe)_2]^{2+}$ and $[HCO_2]^-$ (δ 8.40) was observed. Addition of just a single equivalent of borane promoted 60% conversion to $[HCO_2]^-$ (δ 8.29), consistent with a much larger K_{eq} (in different units). Addition of 10 equiv borane led to essentially complete conversion to

$[Ni(dmpe)_2]^{2+}$ and $[HCO_2]^-$ (δ 8.22). Accurate values for the equilbrium constants have not yet been measured.

Addition of one equivalent of $[Bu_4N][HCO_2]$ to the mixture at the end of the reaction led to an essentially negligible (0.003 ppm) shift in the $[HCO_2]^-$ resonance while the peak intensity and integration roughly doubled, indicating that the resonance between δ 8.2 and 8.4 was indeed formate. The origin of the formate was conclusively shown to be CO_2 by reaction of $[HNi(dmpe)_2][PF_6]$ with one equiv $^{13}CO_2$, which produced a 202 Hz doublet, δ 8.21, in the ^1H NMR spectrum, along with an intense resonance, δ 174.16, in the $^{13}C\{^1H\}$ NMR spectrum. The ^{11}B NMR resonance of the borane in CD_3CN is far upfield of the resonance in C_6D_5Cl, consistent with CD_3CN adduct formation. This must be reversible, however, as the ^{11}B NMR resonance shifts further upfield by ~3 ppm as formate is produced. A formate-borane adduct is also evidenced by shifts in ^1H NMR resonances of the borane and formate as the reaction proceeds. Borane adduct formation with formate must be significantly stronger than adduct formation with CD_3CN. The ready availability of $[HNi(dmpe)_2][PF_6]$ from H_2 with a suitable base such as NEt_3 suggests a net transformation of H_2 and CO_2 to $[HNEt_3][HCO_2]$ using a Ni species and Lewis acid assistance.

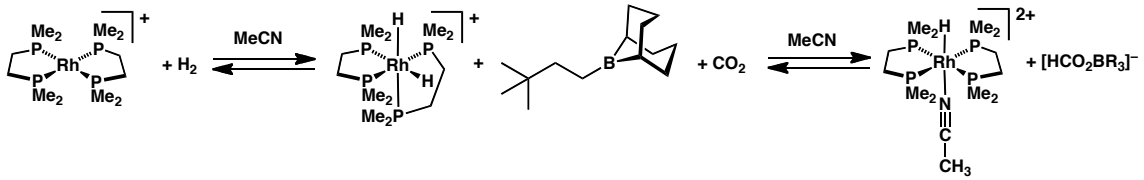

Scheme 5.10

Hydrogen could be used directly for CO_2 reduction by employing the rhodium cation $[Rh(dmpe)_2][OTf]$. Treatment of $[Rh(dmpe)_2][OTf]$ with a mixture of H_2 and CO_2 (1 atm total) in CD_3CN led to formation of some $[H_2Rh(dmpe)_2][OTf]$ (ΔG_{H^-} = 50.4 kcal mol^{-1}),[14] but no formate production over 4 days. Inclusion of ^{t}Bu$(CH_2)_2$B(C_8H_{14}) in the reaction led to the observation of formate over a few hours (δ 8.24) in addition to the Rh product of hydride transfer, $[HRh(dmpe)_2(MeCN)]^{2+}$ (Scheme 5.10). With one equivalent of borane, the reaction yielded ~25% formate. Some $[Rh(dmpe)_2]^+$ remained during the course of the reaction, consistent with H_2 oxidative addition being uphill by 0.44 kcal mol^{-1}.[14] Under 1 atm H_2 complete conversion is observed, but only ~0.5 atm H_2 is present at the start of these reactions. The similarity of the borane/formate chemical shifts in the Ni and Rh reactions suggests that adduct formation does not involve the metal center.

With the help of even small amounts of the appropriate borane Lewis acid, the Rh dihydride (with similar hydride strength to $[HNi(dmpe)_2]^+$) can utilize H_2 directly to reduce CO_2 under very mild conditions of pressure and temperature, and without the need for external base additives. The resulting Rh dication, $[HRh(dmpe)_2(MeCN)]^{2+}$, has a pK_a almost identical to $[HNEt_3]^+$ in MeCN (18.9[14] and 18.8,[15] respectively).

Attempted catalysis and dihydrogen cleavage solvent dependence

In order to achieve a catalytic reaction in nickel, a suitable base such as NEt_3[12d] must cleave H_2 in concert with $[Ni(dmpe)_2]^{2+}$, followed by hydride delivery to CO_2. All of the reagents are compatible with each other; sufficient steric bulk is required to avoid stable Lewis adduct formation. A mixture of $[Ni]^{2+}$, 4 equiv NEt_3, and 4 equiv BEt_3 were subjected to a

1:1 mixture of H_2/CO_2 (1 atm) in CD_3CN, and slow conversion to small amounts of formate was observed. Only ~8% formate relative to Ni was observed over 3 days; but this non-catalytic reaction confirmed that even $[Ni(dmpe)_2]^{2+}$ can moderate CO_2 reduction using H_2 (and NEt_3) directly. Formation of $[HNi(dmpe)_2]^+$ is extremely slow in these conditions, perhaps accounting for the problems; a mixture of $[Ni(dmpe)_2][PF_6]_2$ and NEt_3 (4 equiv) was only 30% converted to $[HNi(dmpe)_2][PF_6]$ after 3 days under 1 atm H_2.

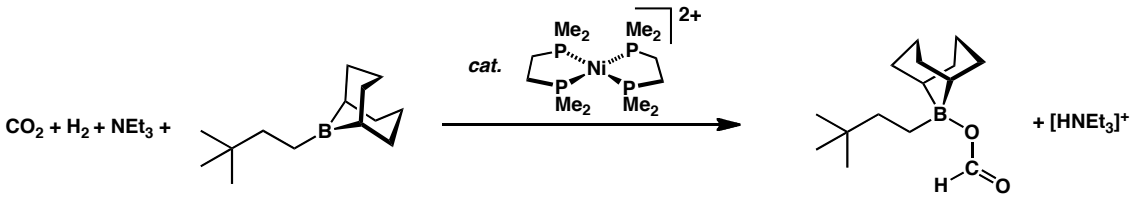

Scheme 5.11

Frustrated by the sluggish H_2 cleavage reactivity of $[Ni(dmpe)_2][PF_6]_2$ in CD_3CN, we generated $[Ni(dmpe)_2][BAr^F{}_4]_2$ and tested the reactivity in C_6D_5Cl. Surprisingly, the reaction of $[Ni(dmpe)_2][BAr^F{}_4]_2$ and NEt_3 with H_2 proceeded far faster in C_6D_5Cl, with high conversion to $[HNi(dmpe)_2]^+$ in 3 hours, and full conversion after 18 hours.

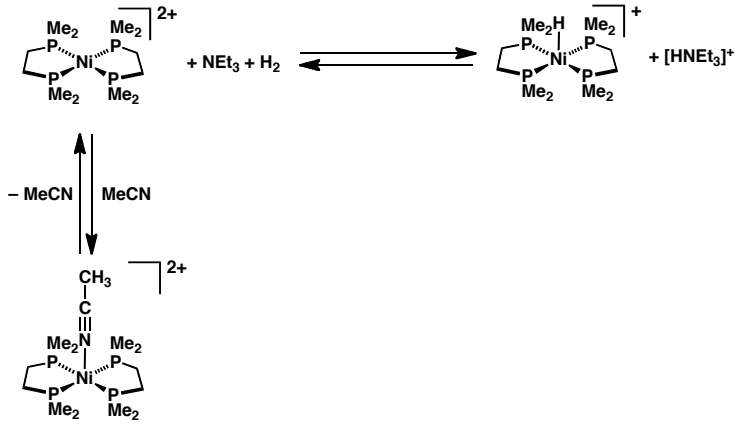

Scheme 5.12

It is exciting that the slow kinetics of H_2 cleavage are not a result of any implicit characteristic of $[Ni(dmpe)_2]^{2+}$, but rather appear to be a problem unique to acetonitrile solutions. Waiting days for hydride formation would preclude the use of bis(diphosphine)nickel complexes in any practical applications; the use of non-coordinating solvents makes these nickel hydride delivery reagents more relevant (and able to compete with more expensive Pt analogues in terms of rates). Anion effects were discounted by placing $[Ni(dmpe)_2][BAr^F{}_4]_2$ and NEt_3 under H_2 in CD_3CN, which proceeded at roughly the same rate as heterolytic cleavage by $[Ni(dmpe)_2][PF_6]_2$. We ascribe the slow heterolytic cleavage of H_2 in CD_3CN to solvent inhibition, as shown in Scheme 5.12: the 5-coordinate 18 e^- MeCN adduct $[Ni(dmpe)_2(MeCN)]^{2+}$ has been structurally characterized,[12a] and dissociation of MeCN would be inhibited by the solvent. DuBois estimated $K_{eq} = 0.3$ for adduct formation using electrochemical techniques. While this equilibrium must be dealt with in MeCN solutions, in chlorobenzene no donor binds the axial position of the square planar Ni (a structure of 4-coordinate $[Ni(dmpe)_2]^{2+}$ is also known)[12a]. Bis(diphosphine)platinum dications do not form 5-coordinate species in acetonitrile, accounting for the difference in reactivity between Ni and Pt in that solvent.

Catalytic conditions similar to those in acetonitrile were employed, and despite the steady growth of $[HNi(dmpe)_2]^+$ over a few days, the reaction did not produce any detectable formate. Reactions in the more commonly used solvent CD_2Cl_2 were also briefly explored, but formation of CD_2HCl was observed, indicating a hydride transfer side reaction. It is unclear why no formate is observed in chlorobenzene, especially in light of the partial conversion in CD_3CN. One possibility is that while the H_2 cleavage reaction is enhanced by

the BAr^{F}_{4} counterions, the hydride transfer reaction is slowed, as observed for CO reduction.[10d]

Conclusions

Partially reduced rhenium carbonyl species and late transition metal bis(diphosphine) hydrides both reduce carbon dioxide to formate. The trialkylborane groups that promote key steps in CO reduction are also crucial to the observed CO_2 reduction reactivity. Borane-formate adduct formation is likely responsible for the favorable shift in equilibrium towards formate products. Encouragingly, the borane-formate adduct is relatively weakly bound (as judged by NMR spectroscopy), which raises the promise of such additives being useful in catalytic systems. While catalysis has so far eluded us, we have also shown that H_2 and CO_2 can be used directly in Ni and Rh systems to produce the borane-formate adduct; notably, these systems are unable to reduce more than a trace amount of CO_2 in the absence of an appropriate Lewis acid. The dihydrogen cleavage step required for catalysis was also briefly explored, and the judicious choice of anion and solvent can greatly accelerate the heterolytic cleavage of dihydrogen by bis(diphosphine)nickel dications. The reported improvements in dihydrogen cleavage, coupled with a new gentle strategy for promoting CO_2 reduction by hydride transfer, point towards a practical catalytic CO_2 hydrogenation system based on a nickel.

Experimental Section

General Considerations

All air- and moisture-sensitive compounds were manipulated using standard vacuum line or Schlenk techniques, or in a glovebox under a nitrogen atmosphere. Under standard glovebox conditions, petroleum ether, diethyl ether, benzene, toluene, and tetrahydrofuran were used without purging, such that traces of those solvents were in the atmosphere, and could be found intermixed in the solvent bottles. The solvents for air- and moisture-sensitive reactions were dried over sodium benzophenone ketyl, calcium hydride, or by the method of Grubbs.[16] All NMR solvents were purchased from Cambridge Isotopes Laboratories, Inc. Chlorobenzene-d_5 (C_6D_5Cl) and dichloromethane-d_2 (CD_2Cl_2) were freeze–pump–thaw degassed three times before being run through a small column of activated alumina. Tetrahydrofuran-d_8 (THF-d_8) was purchased in a sealed ampoule, and dried by passage through activated alumina. Unless noted, other materials were used as received. [**1**][BF_4][10a] **2**, [Pt(dmpe)$_2$][PF_6]$_2$,[11] [HPt(dmpe)$_2$][PF_6],[11] [Ni(dmpe)$_2$][BF_4]$_2$,[12a] [HNi(dmpe)$_2$][PF_6],[11] ^{t}Bu(CH_2)$_2$B(C_8H_{14}),[17] [Bu_4N][HCO_2],[18] [Ni(dmpe)$_2$][$BAr^F{}_4$]$_2$,[10c] and [Rh(dmpe)$_2$][OTf][12h,14] were synthesized by literature methods. All other materials were readily commercially available, and used as received. ^{1}H and ^{13}C NMR spectra were recorded on Varian Mercury 300 MHz, or Varian INOVA-500 or 600 MHz spectrometers at room temperature, unless indicated otherwise. Chemical shifts are reported with respect to residual internal protio solvent for ^{1}H and ^{13}C{^{1}H} spectra. Other nuclei were referenced to an external standard: H_3PO_4 (^{31}P), 15% BF_3•Et_2O/$CDCl_3$ (^{11}B), $CFCl_3$ (^{19}F), all at 0 ppm.

Experimental Procedures

Reaction of 2 with CO_2. A 10 mL vial was charged with 26.4 mg (0.0251 mmol) [**1**][BF_4] and ~0.6 mL C_6D_5Cl. With stirring, 25.1 μL (0.0251 mmol) $NaHBEt_3$ (1.0 M in toluene) was added dropwise to provide a pale yellow solution. The reaction mixture was transferred to a J-Young NMR tube and initial spectroscopic measurements showed clean conversion to boroxycarbene **2**. The tube was placed under vacuum for 1 minute with gentle shaking to degas, and one atmosphere of CO_2 was then admitted to the tube. NMR spectroscopy after 5 minutes showed complete conversion to a new product, most of which precipitated overnight. **^{1}H NMR** (C_6D_5Cl, 500 MHz): toluene and BEt_3 are omitted, but overlap with some aliphatic peaks, preventing good integration. δ 0.69 (br s, 4H), 1.59 (br s, overlapping), 1.84 (br, overlapping), 2.05 (br m, overlapping), 2.73 (br, 4H), 7.41 (br, 12H), 8.45 (s, 1H, *H*CO_2^-). **^{31}P{^{1}H} NMR** (C_6D_5Cl, 121 MHz): δ 2.2. **IR** (C_6D_5Cl): ν_{CO}1993, 1620 cm^{-1}.

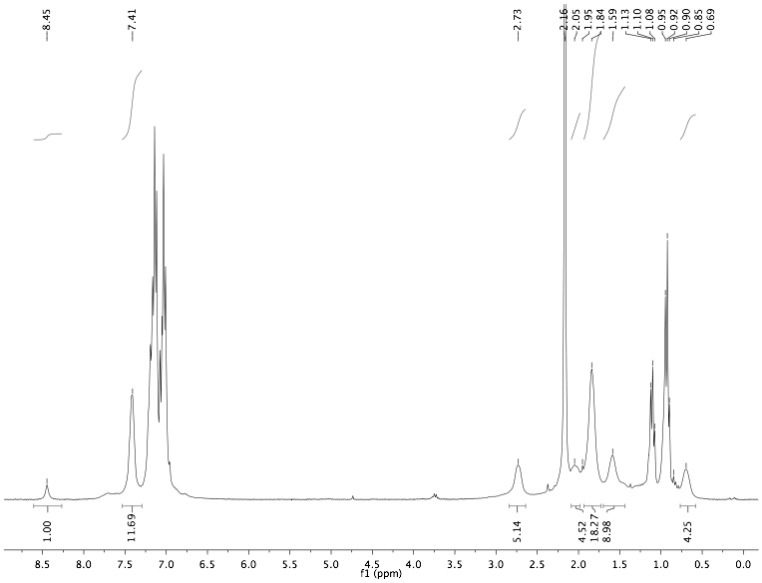

Figure 5.2. ^{1}H NMR of **1**•(HCO_2).

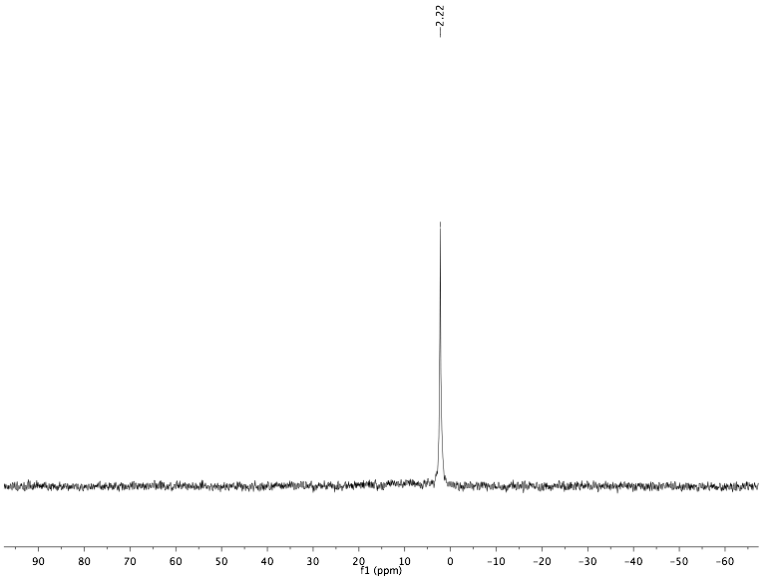

Figure 5.3. $^{31}P\{^{1}H\}$ NMR of **1**•(HCO_2).

Reaction of [1][BF_4] with [Bu_4N][HCO_2]. A J-Young NMR tube was charged with 29.1 mg (0.0276 mmol) [**1**][BF_4], 7.9 mg (0.0276 mmol) [Bu_4N][HCO_2], and ~0.6 mL C_6D_5Cl. After 15 minutes, ^{1}H and $^{31}P\{^{1}H\}$ NMR spectroscopy showed essentially complete conversion to **1**•(HCO_2). After about 30 minutes, some precipitates were

observed, and precipitation of white solids continued over the next 3 hours. At this time, the solution was decanted, and IR spectroscopy showed resonances that matched the preparation of **1**•(HCO_2) from CO_2; an additional peak at 1660 cm^{-1} is unidentified, however. **^{1}H NMR** (C_6D_5Cl, 400 MHz): $[Bu_4N]^+$ peaks omitted. δ 0.68 (br, 4H), 0.95 (br, 4H), 1.58 (br, 4H), 1.83 (br, 16H), 2.03 (br, 4H), 2.75 (br, 4H), 7.1-7.2 (m, 12H), 7.4 (m, 8H), 8.49 (s, 1H, $[HCO_2]^-$). **^{31}P{^{1}H} NMR** (C_6D_5Cl, 162 MHz): δ 2.4. IR (C_6D_5Cl): 1993, 1660, 1621 cm^{-1}.

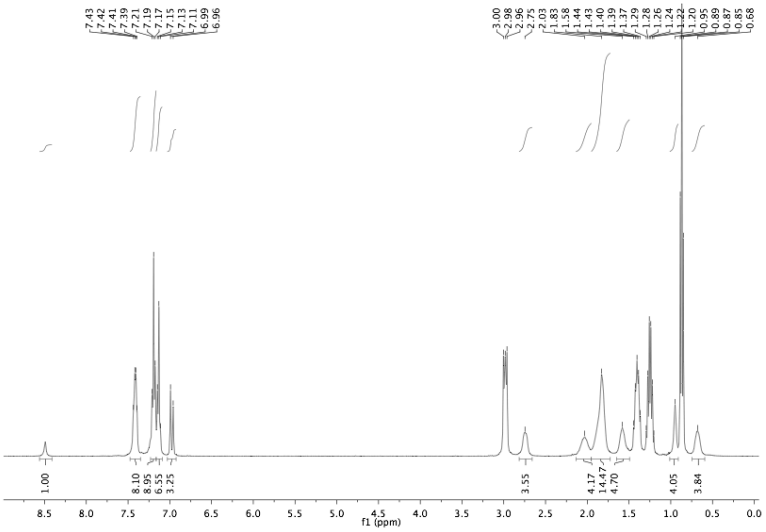

Figure 5.4. ^{1}H NMR of **1**•(HCO_2) (from $[Bu_4N][HCO_2]$).

Reaction of [1][BF_4] and [HNi(dmpe)$_2$][PF_6] with CO_2 in C_6D_5Cl. A J-Young NMR tube was charged with 24.3 mg (0.0231 mmol) [**1**][BF_4], 11.6 mg (0.0231 mmol) [HNi(dmpe)$_2$][PF_6], and ~0.6 mL C_6D_5Cl. The tube was sealed and initial NMR spectroscopic measurements were made which showed no reaction, at which point 1 atm CO_2 was added. After ~20 minutes some formate was observed, which grew in over a few hours. During this time precipitates formed, and after about 12 hours there was essentially

no formate-containing products in solution. The solids were collected, and washed with CD_3CN (which extracted $[Ni(dmpe)_2][PF_6]_2$) and C_6D_5Cl. Then the solids were treated with C_6D_5Cl and 3.8 μL (0.0462 mmol, 2 equiv) pyridine, which prompted the majority of the solids to dissolve. An asymmetric product was observed by NMR which was assigned as **1**•(HCO_2)(pyridine).

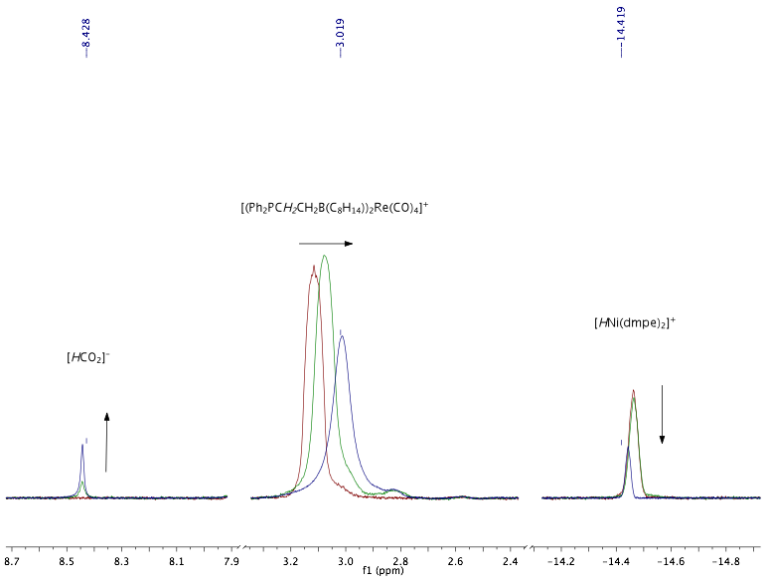

Figure 5.5. Time course (^{1}H NMR excerpts) of reaction of [**1**]$^+$ with $[HNi(dmpe)_2]^+$ and CO_2.

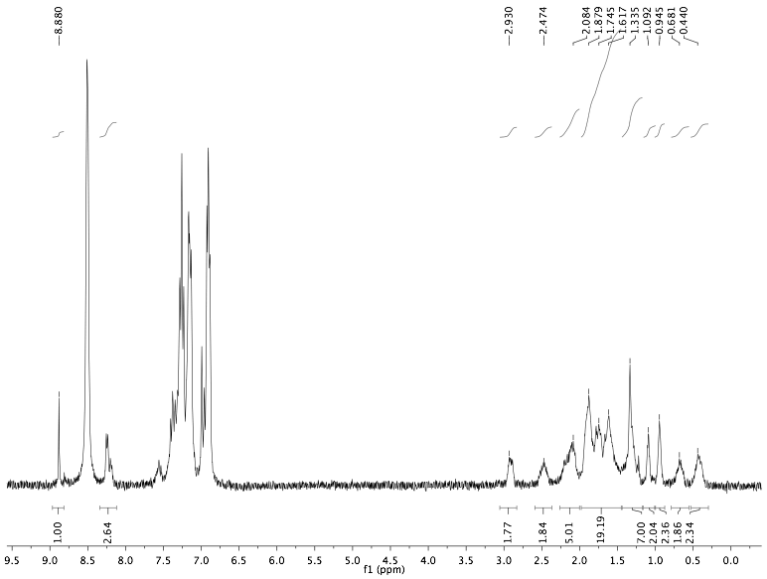

Figure 5.6. ^{1}H NMR of **1**•(HCO_2)(pyridine).

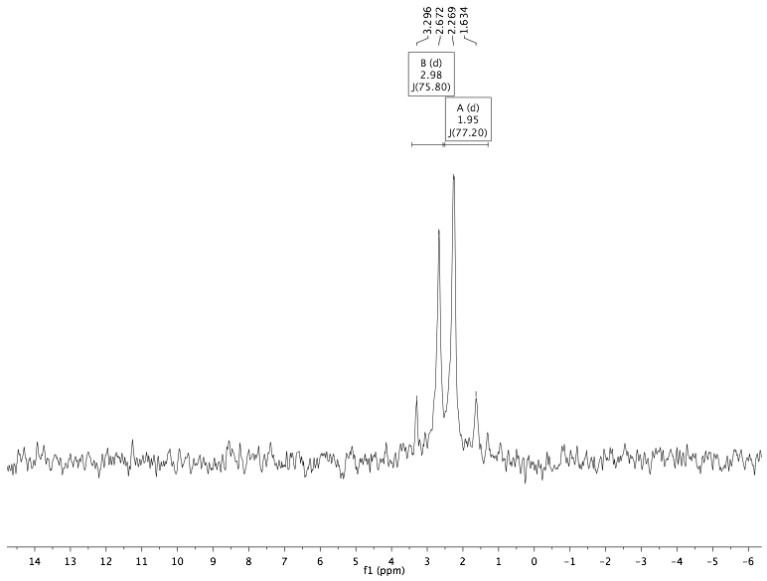

Figure 5.7. $^{31}P\{^{1}H\}$ NMR of **1**•(HCO_2)(pyridine).

Reactions in chlorobenzene

Reaction of [HNi(dmpe)$_2$][PF$_6$] with ^{t}Bu(CH$_2$)$_2$B(C$_8$H$_{14}$) and CO$_2$. A ~0.6 mL C_6D_5Cl solution of 6.7 mg (0.0327 mmol) ^{t}Bu(CH_2)$_2$B(C_8H_{14}) was added to 16.5 mg (0.0327

mmol) solid $[HNi(dmpe)_2][PF_6]$. The reaction mixture was transferred to a J-Young NMR tube, and initial spectroscopic measurements were made. After two freeze–pump–thaw cycles, 1 atm CO_2 was admitted to the tube, and the reaction was monitored by NMR spectroscopy. After 24 hours the reaction had reached partial conversion, which did not change over 4 days. Addition of 16.0 mg (0.0327 mmol) $[hept_4N][Br]$ led to essentially complete conversion to $[hept_4N][HCO_2BR_3]$.

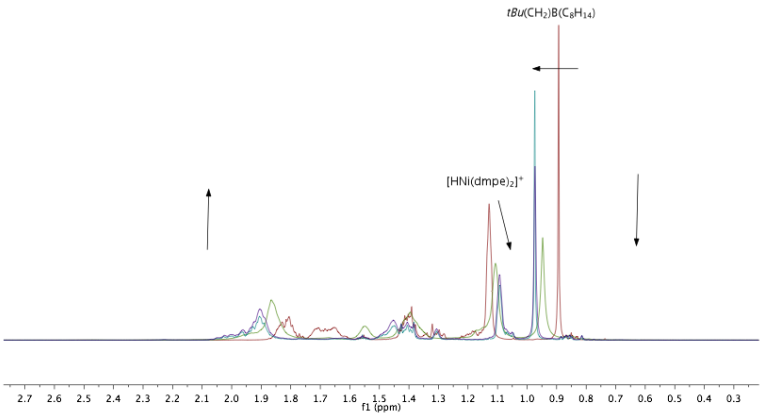

Figure 5.8. Time course (^{1}H NMR alkyl region) of reaction of $[HNi(dmpe)_2]^+$ with ^{t}Bu$(CH_2)_2B(C_8H_{14})$ and CO_2.

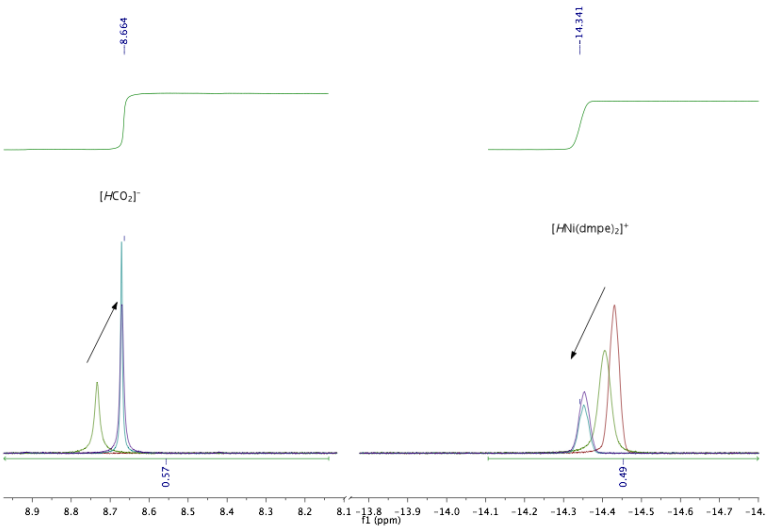

Figure 5.9. Time course (^{1}H NMR formate and hydride region) of reaction of $[HNi(dmpe)_2]^+$ with ^{t}Bu$(CH_2)_2$B(C_8H_{14}) and CO_2.

General procedure for reactions of [HNi(dmpe)$_2$][PF$_6$] with other boranes. A ~0.6 mL C_6D_5Cl solution of borane (~0.03 mmol) was added to an equimolar amount of solid $[HNi(dmpe)_2][PF_6]$. The reaction mixture was transferred to a J-Young NMR tube, and initial spectroscopic measurements were made. After two freeze–pump–thaw cycles, 1 atm CO_2 was admitted to the tube, and the reaction was monitored by NMR spectroscopy.

Isopropyl pinacol borate. The reaction proceeded essentially the same as that with no borane added. The formate resonance appears between δ 8.70 and 8.74 during the reaction, significantly upfield of $[Bu_4N][HCO_2]$ (δ 9.58) and the trace formate produced in acid-free reaction (δ 8.84), but downfield of the reaction with ^{t}Bu$(CH_2)_2$B(C_8H_{14}) (δ 8.66); this could be due to a weak B–O interaction or effects related to the identity of the counter cation.

Triphenylborane. A presumed formate resonance is visible at 8.8 ppm by ^{1}H NMR, along with some unidentified peaks between 5 and 6 ppm. The phenyl region of BPh_3 suggests formation of multiple products, and essentially complete transfer of $[HNi(dmpe)_2]^+$ is observed.

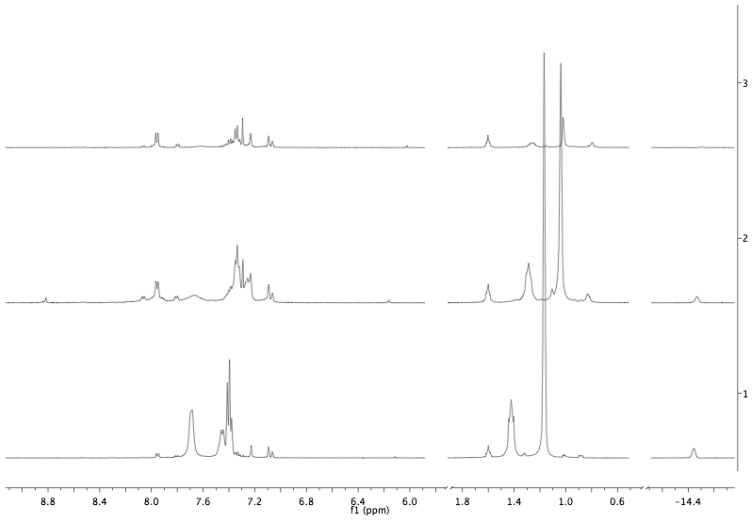

Figure 5.10. Reaction of $[HNi(dmpe)_2]^+$ and BPh_3 before CO_2 addition (bottom); 5 hours after addition (middle); 2 days after addition (top).

Trimesitylborane. No change in reactivity was observed as compared to the reaction without borane. Formate chemical shift (δ 8.63) was, however, similar to the reaction with ^{t}Bu$(CH_2)_2$B(C_8H_{14}) (δ 8.66).

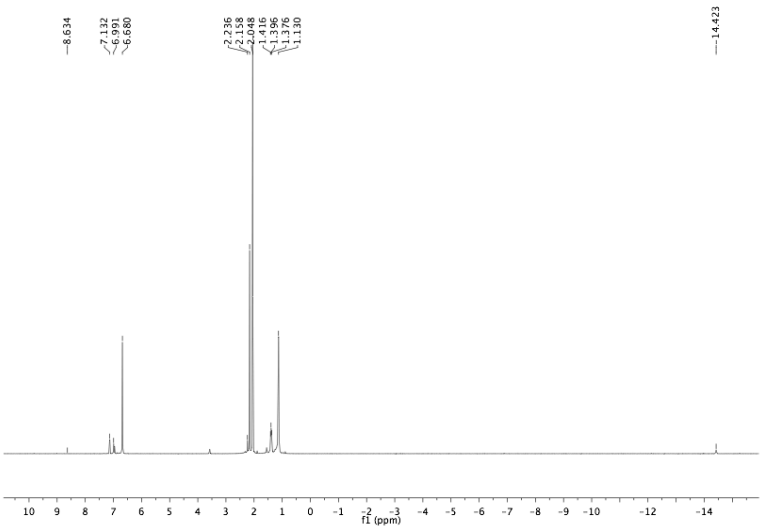

Figure 5.11. ^{1}H NMR of mixture of $[HNi(dmpe)_2]^+$, $BMes_3$, and CO_2.

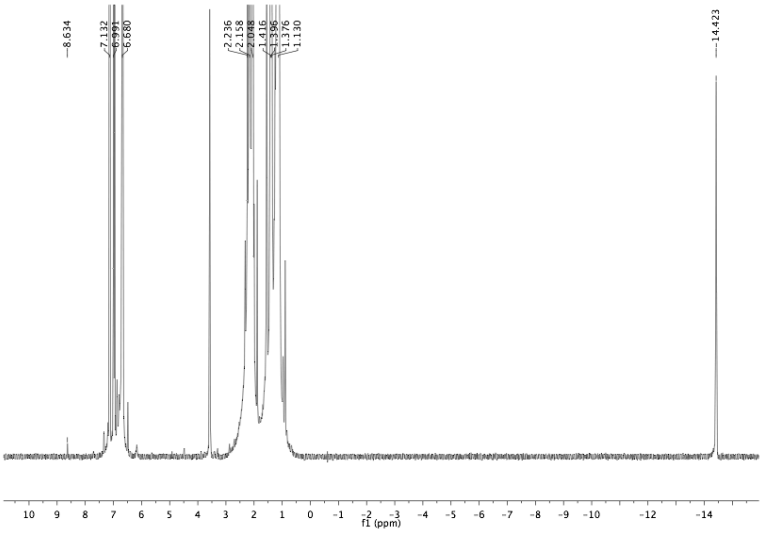

Figure 5.12. ^{1}H NMR (blow-up) of mixture of $[HNi(dmpe)_2]^+$, $BMes_3$, and CO_2.

$B(C_6F_5)_3$. This reaction appears to result in hydride abstraction to form $[HB(C_6F_5)_3]^-$. The ^{19}F NMR is consistent with a 4-coordinate borate environment, and complete comsumption of $B(C_6F_5)_3$ (some $[HNi(dmpe)_2]^+$ was left over due to poor stoichiometry); ^{11}B NMR is also consistent, although the resonance is slightly downfield from the expected chemical shift of $[HB(C_6F_5)_3]^-$, and the resonance is broadened beyond being able to

observe coupling. This could be due to exchange with some free borane or with the Ni if the reaction is reversible. Even if CO_2 is added after this point, no formate was observed overnight at room temperature. Heating to 100 °C resulted in a small amount of formate, consistent with hydride transfer from either the small amount of remaining $[HNi(dmpe)_2]^+$ or from $[HB(C_6F_5)_3]^-$ as reported by Ashley et al.[8]

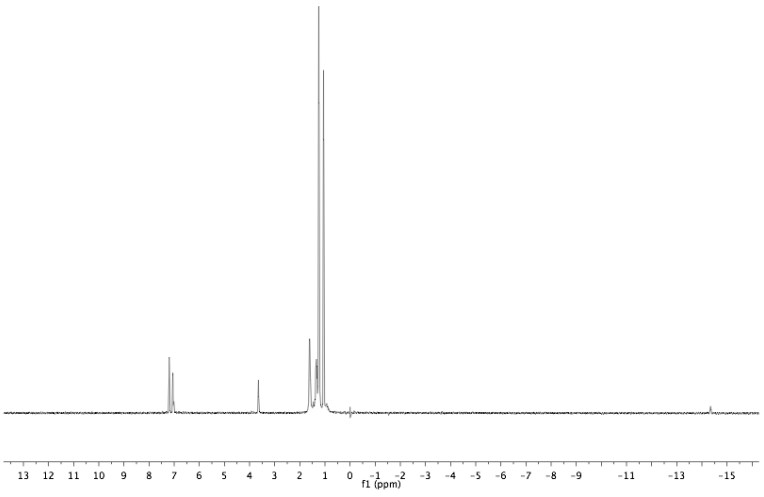

Figure 5.13. ^1H NMR of reaction of $[HNi(dmpe)_2]^+$ with $B(C_6F_5)_3$ and CO_2.

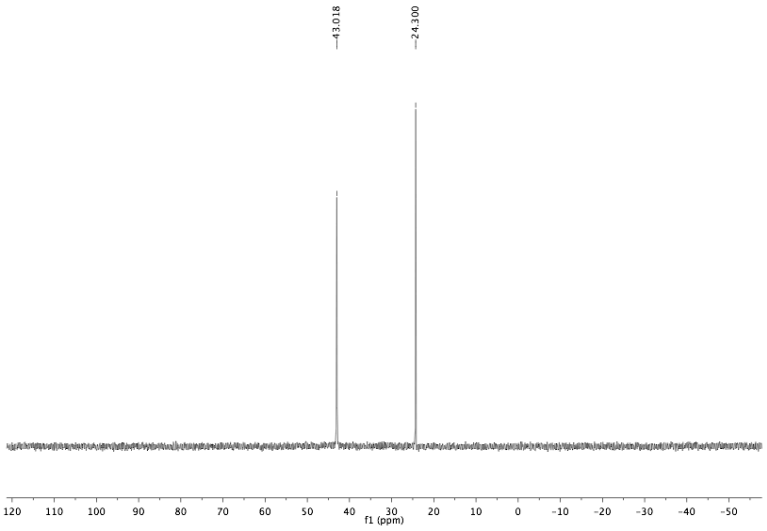

Figure 5.14. $^{31}P\{^{1}H\}$ NMR of reaction of $[HNi(dmpe)_2]^+$ with $B(C_6F_5)_3$ and CO_2.

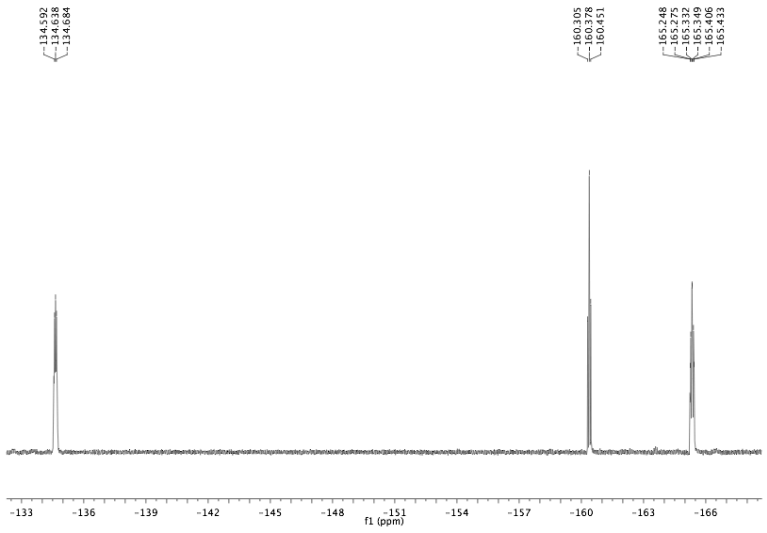

Figure 5.15. ^{19}F NMR of reaction of $[HNi(dmpe)_2]^+$ with $B(C_6F_5)_3$ and CO_2.

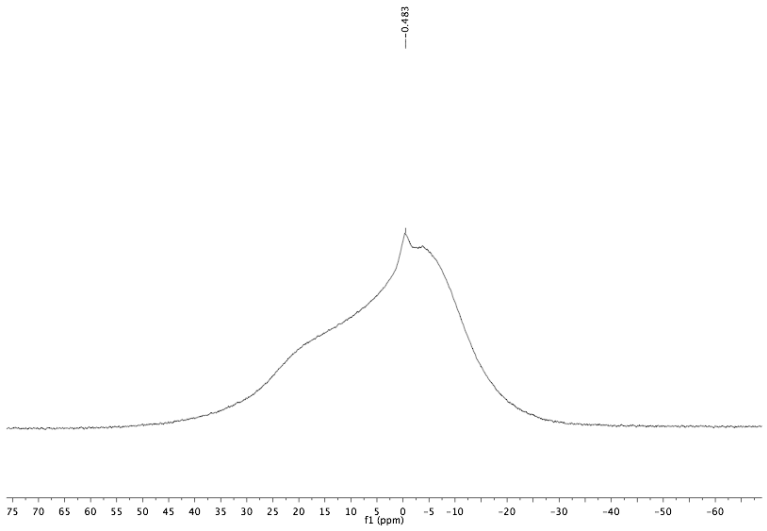

Figure 5.16. ^{11}B NMR of reaction of $[HNi(dmpe)_2]^+$ with $B(C_6F_5)_3$ and CO_2.

Reaction of $[Bu_4N][HCO_2]$ with ^{t}Bu$(CH_2)_2$B(C_8H_{14}) in C_6D_5Cl. A J-Young NMR tube was charged with 15.8 mg (0.0549 mmol) $[Bu_4N][HCO_2]$, 11.3 mg (0.0549 mmol) ^{t}Bu$(CH_2)_2$B(C_8H_{14}), and ~0.6 mL C_6D_5Cl. NMR spectroscopy revealed a formate resonance at δ 8.89, well upfield of $[Bu_4N][HCO_2]$ in the absence of borane (δ 9.58). The broad ^{11}B signal appears to be around δ 2.7. **^{1}H NMR** (C_6D_5Cl, 500 MHz): δ 0.76 (m, ^{t}BuCH$_2$C*H$_2$*B(C_8H_{14}), 2H), 0.86 (t, J = 7.3 Hz, N$(CH_2CH_2CH_2CH_3)_4$, 12H), 1.04 (s, ^{t}*Bu*CH$_2$CH$_2$B(C_8H_{14}), 9H), 1.25 (q, J = 7.2 Hz, N$(CH_2CH_2CH_2CH_3)_4$, 8H), 1.4 (m, 10H, N$(CH_2CH_2CH_2CH_3)_4$ and ^{t}BuC*H$_2$*CH$_2$B(C_8H_{14}) overlapping), 1.83 (br, ^{t}BuCH$_2$CH$_2$B(C_8H_{14}), 2H), 1.97 (br, ^{t}BuCH$_2$CH$_2$B(C_8H_{14}), 4H), 2.28 (br, ^{t}BuCH$_2$CH$_2$B(C_8H_{14}), 6H), 3.00 (m, N$(CH_2CH_2CH_2CH_3)_4$), 8.89 (s, HCO_2^-, 1H). **^{13}C{^{1}H} NMR** (C_6D_5Cl, 126 MHz): δ 13.66, 19.87, 23.91, 26.80, 30.05, 31.35, 33.0 (br), 40.75, 58.66, 168.48. **^{11}B NMR** (C_6D_5Cl, 160 MHz): δ 2.7.

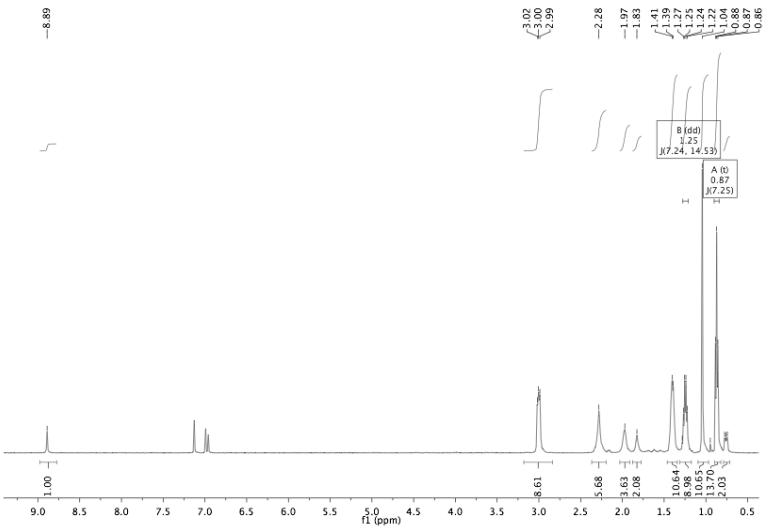

Figure 5.17. ^{1}H NMR of $[Bu_4N][HCO_2BR_3]$.

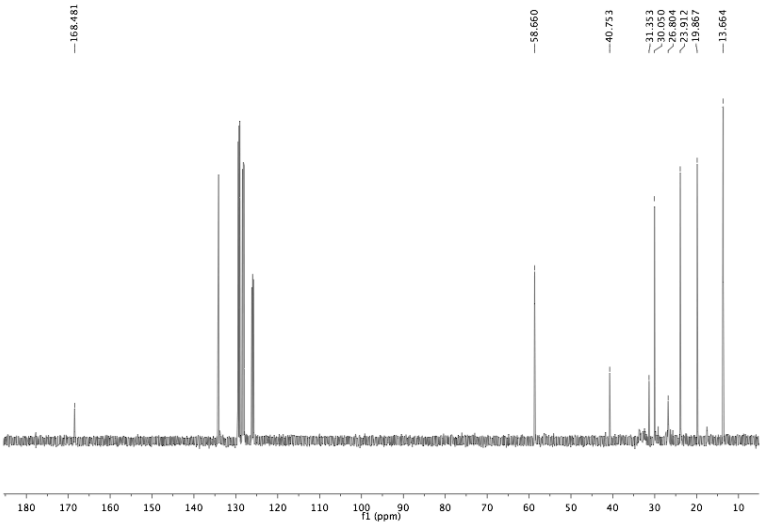

Figure 5.18. $^{13}C\{^{1}H\}$ NMR of $[Bu_4N][HCO_2BR_3]$.

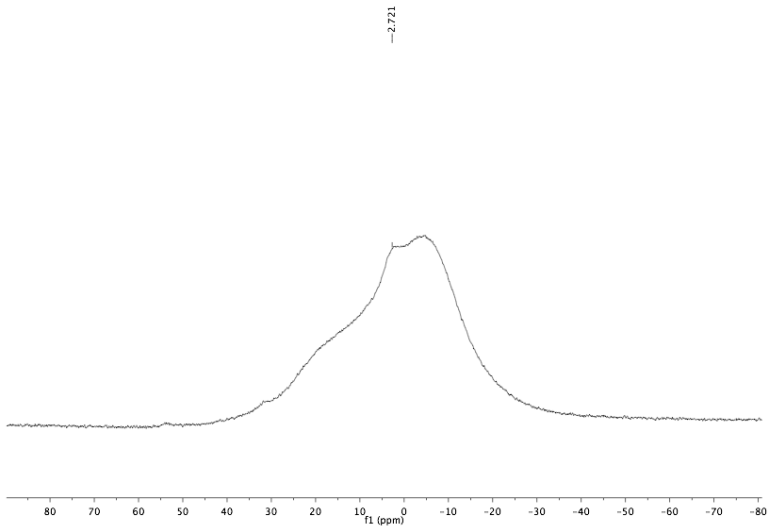

Figure 5.19. ^{11}B NMR of $[Bu_4N][HCO_2BR_3]$.

General procedure for reactions of $[HNi(dmpe)_2][PF_6]$ in acetonitrile. A J-Young NMR tube was charged with $[HNi(dmpe)_2][PF_6]$ (~0.03 mmol), the appropriate amount of $^tBu(CH_2)_2B(C_8H_{14})$ (0, 1, 10 equiv), and ~0.6 mL C_6D_5Cl. The tube was sealed, initial NMR measurements were taken, and the atmosphere replaced with 1 atm CO_2 (after freeze–pump–thaw degassing twice). The reactions were monitored periodically by multinuclear NMR until equilibrium was reached (under 24 hours). The spectra at equilibrium are overlaid below.

CO_2. About 5% hydride transfer was observed.

1 equiv $^tBu(CH_2)_2B(C_8H_{14})$ and CO_2. About 65% hydride transfer was observed.

10 equiv $^tBu(CH_2)_2B(C_8H_{14})$ and CO_2. Nearly quantitative hydride transfer was observed.

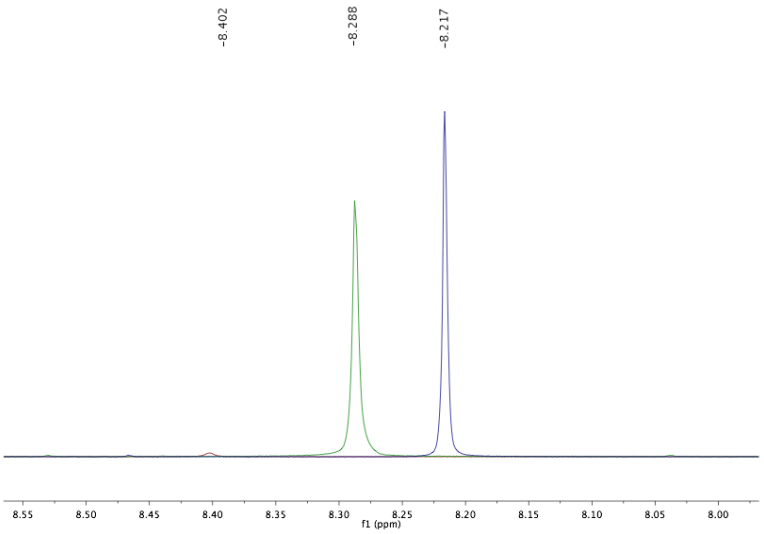

Figure 5.20. Overlay (^{1}H NMR, formate region) of equilibrated reactions of $[HNi(dmpe)_2]^+$ with CO_2 and 0 (red), 1 (green) and 10 (blue) equiv ^{t}Bu$(CH_2)_2$B(C_8H_{14}).

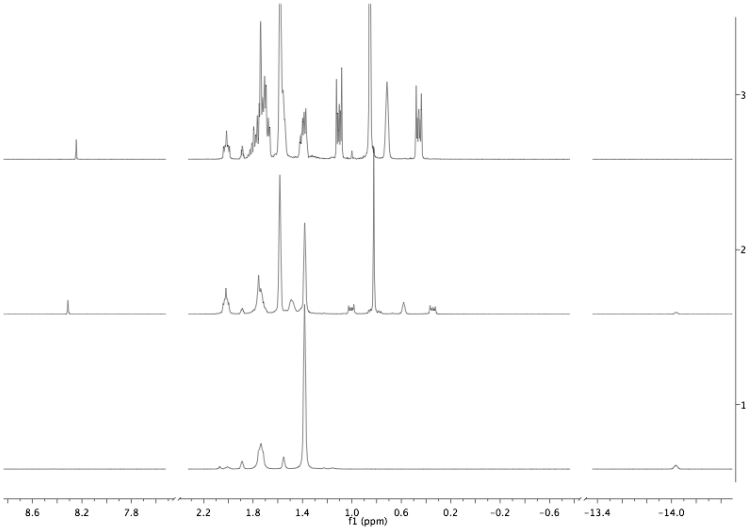

Figure 5.21. Comparison (^{1}H NMR) of equilibrated reactions of $[HNi(dmpe)_2]^+$ with CO_2 and 0 (bottom), 1 (middle) and 10 (top) equiv ^{t}Bu$(CH_2)_2$B(C_8H_{14}).

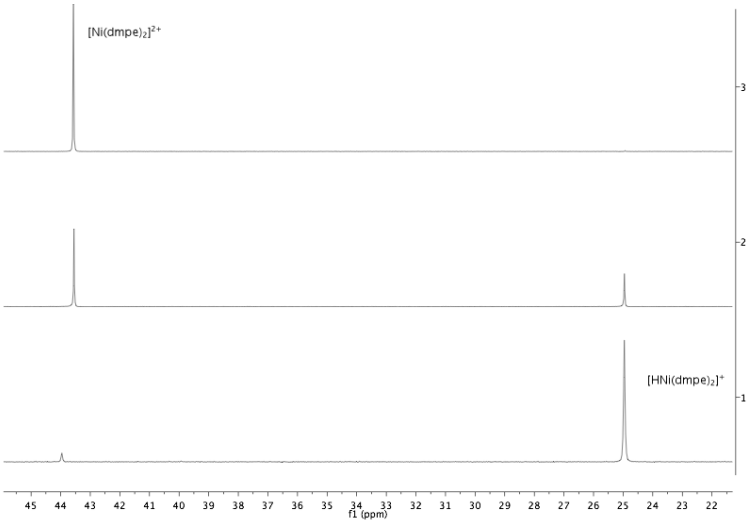

Figure 5.22. Comparison ($^{31}P\{^{1}H\}$ NMR) of equilibrated reactions of $[HNi(dmpe)_2]^+$ with CO_2 and 0 (bottom), 1 (middle) and 10 (top) equiv $^{t}Bu(CH_2)_2B(C_8H_{14})$.

Addition of $[Bu_4N][HCO_2]$. A 1:10 mixture of $[HNi(dmpe)_2][PF_6]$ and $^{t}Bu(CH_2)_2B(C_8H_{14})$ was treated with CO_2 according to the general procedure. After reaction was complete, the tube was brought into a glovebox and 1 equiv $[Bu_4N][HCO_2]$ was added to the tube. The spectra showed a tiny (0.003 ppm) shift in the formate peak, while it grew in intensity, thereby confirming its identity.

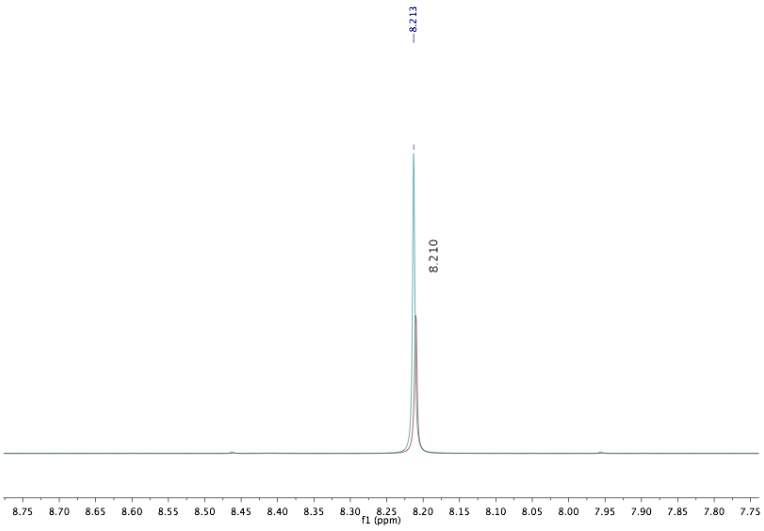

Figure 5.23. ^{1}H NMR (formate region) after reaction of $[HNi(dmpe)_2]^+$ with $^{t}Bu(CH_2)_2B(C_8H_{14})$ and CO_2 (red); after addition of $[Bu_4N][HCO_2]$ (blue).

Reaction with $^{13}CO_2$. A J-Young NMR tube was charged with 18.9 mg (0.0374 mmol) $[HNi(dmpe)_2][PF_6]$, 38.6 mg (0.187 mmol, 5 equiv) $^{t}Bu(CH_2)_2B(C_8H_{14})$, and ~0.6 mL CD_3CN. After initial NMR spectroscopic measurements, the tube was subjected to two freeze–pump–thaw cycles, and 0.0187 mmol (0.5 equiv) $^{13}CO_2$ was condensed from a 2.87 mL calibrated gas bulb (11.8 mmHg). About 5% conversion to $[Ni(dmpe)_2][PF_6]_2$ had occurred after 30 minutes, and a small doublet could be seen by ^{1}H NMR. After 12 hours, a large doublet at δ 8.21 (202 Hz) was visible, consistent with formation of $[H^{13}CO_2]^-$.

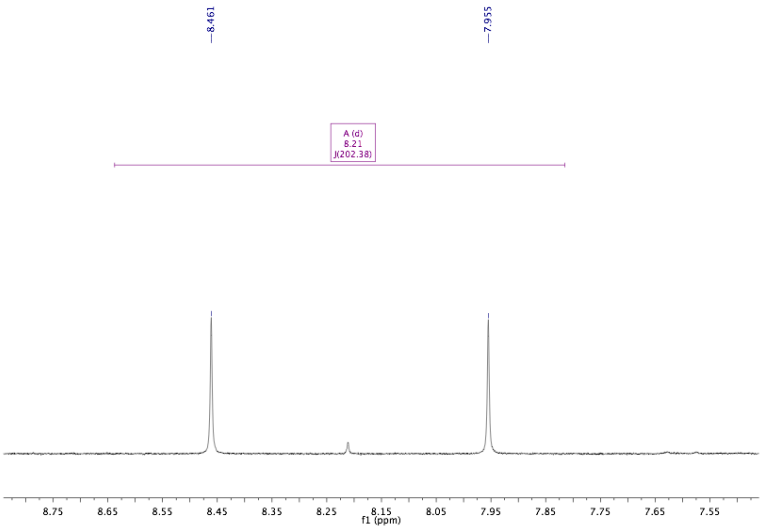

Figure 5.24. 1H NMR (formate region) of reaction of $[HNi(dmpe)_2]^+$ with $^tBu(CH_2)_2B(C_8H_{14})$ and $^{13}CO_2$ (12 hours).

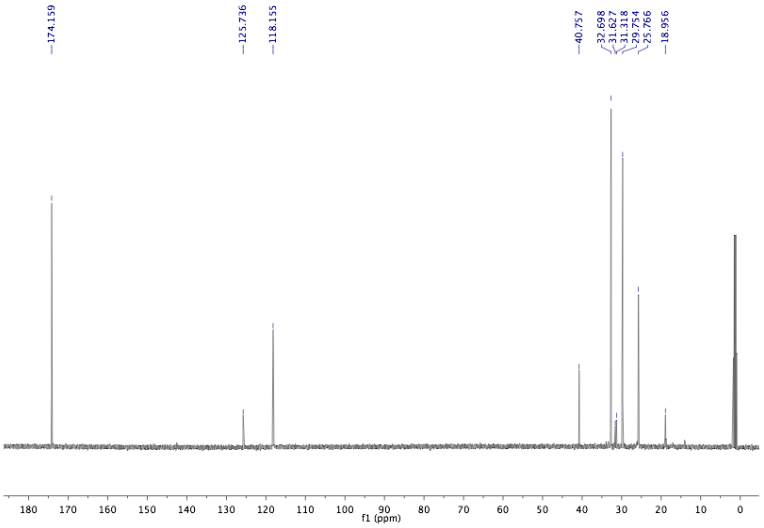

Figure 5.25. $^{13}C\{^1H\}$ NMR of reaction of $[HNi(dmpe)_2]^+$ with $^tBu(CH_2)_2B(C_8H_{14})$ and $^{13}CO_2$ (12 hours).

Reaction of $[Ni(dmpe)_2][PF_6]_2$ with $[Bu_4N][HCO_2]$. A small vial was charged with 19.7 mg (0.0359 mmol) $[Ni(dmpe)_2][PF_6]_2$ and 10.3 mg (0.0359 mmol), and ~0.6 mL CD_3CN. As the mixture was stirred a color change from yellow to dark orange was observed. The mixture was transferred to a J-Young NMR tube, and monitored. The color

faded to a lighter orange over a few minutes. After 15 minutes, almost complete conversion (~95%) to $[HNi(dmpe)_2][PF_6]$ was observed, although a slight excess of $[HCO_2]^-$ was still present.

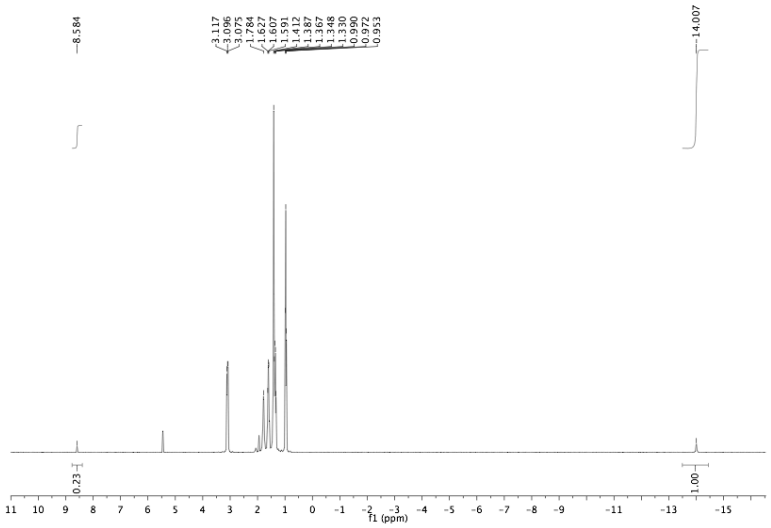

Figure 5.26. ^1H NMR after mixing $[Ni(dmpe)_2][PF_6]_2$ with $[Bu_4N][HCO_2]$.

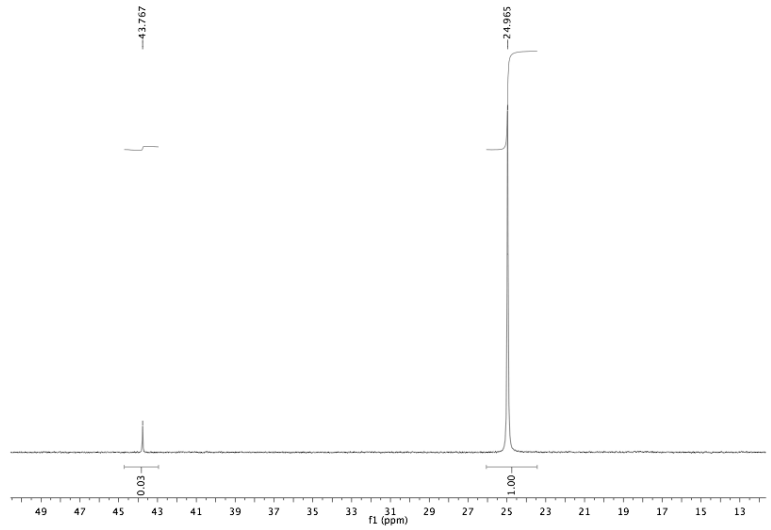

Figure 5.27. $^{31}P\{^1H\}$ NMR after mixing $[Ni(dmpe)_2][PF_6]_2$ with $[Bu_4N][HCO_2]$.

Reaction of $[Rh(dmpe)_2][OTf]$ with H_2 and CO_2. A J-Young NMR tube was charged with 19 mg (0.0344 mmol) $[Rh(dmpe)_2][OTf]$ and ~0.6 mL CD_3CN. The tube

was placed under 1 atm of a 1:1 mixture of H_2 and CO_2, mixed by diffusion in a large round bulb on a vacuum manifold. The reaction was monitored by multinuclear NMR, which showed formation of $[H_2Rh(dmpe)_2][OTf]$, but no more than a trace of formate was observed.

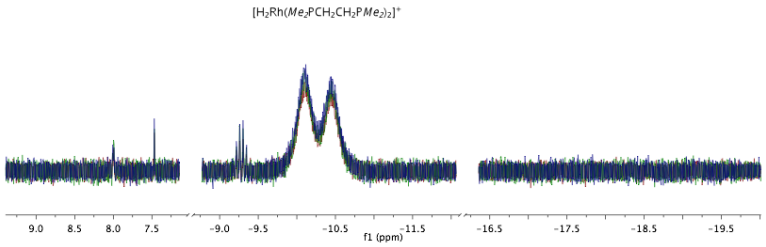

Figure 5.28. ^1H NMR overlay (formate and hydride regions) of reaction of $[Rh(dmpe)_2]^+$ with CO_2 and H_2. After 3 hours (red), 24 hours (green), 4 days (blue).

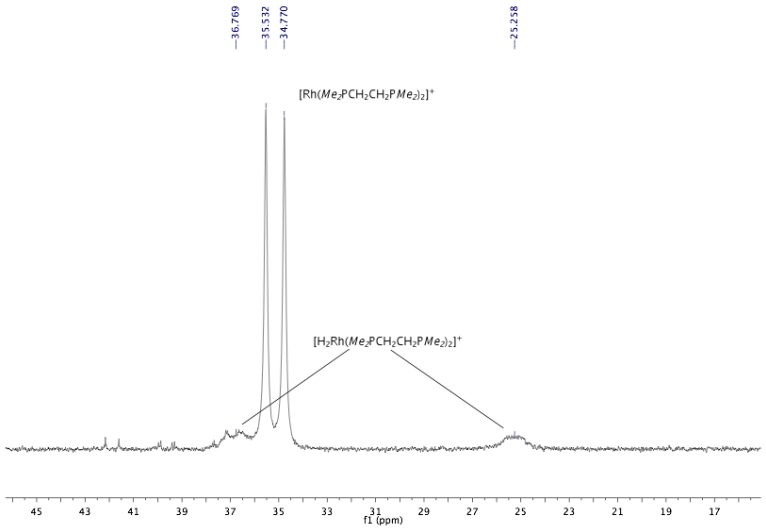

Figure 5.29. $^{31}P\{^1H\}$ NMR of reaction of $[Rh(dmpe)_2]^+$ with CO_2 and H_2 after 24 hours.

Reaction of $[Rh(dmpe)_2][OTf]$ with ^{t}Bu$(CH_2)_2$B(C_8H_{14}) and H_2/CO_2. A J-Young NMR tube was charged with 15.9 mg (0.0288 mmol) $[Rh(dmpe)_2][OTf]$, 5.9 mg (0.0288 mmol) ^{t}Bu$(CH_2)_2$B(C_8H_{14}), and ~0.6 mL CD_3CN. The tube was placed under 1 atm of a

1:1 mixture of H_2 and CO_2, mixed by diffusion in a large round bulb on a vacuum manifold. The reaction was monitored by NMR spectroscopy, which showed growth of signals attributable to $[H_2Rh(dmpe)_2]^+$, and eventually $[HCO_2]^-$ and $[HRh(dmpe)_2(MeCN)]^{2+}$.

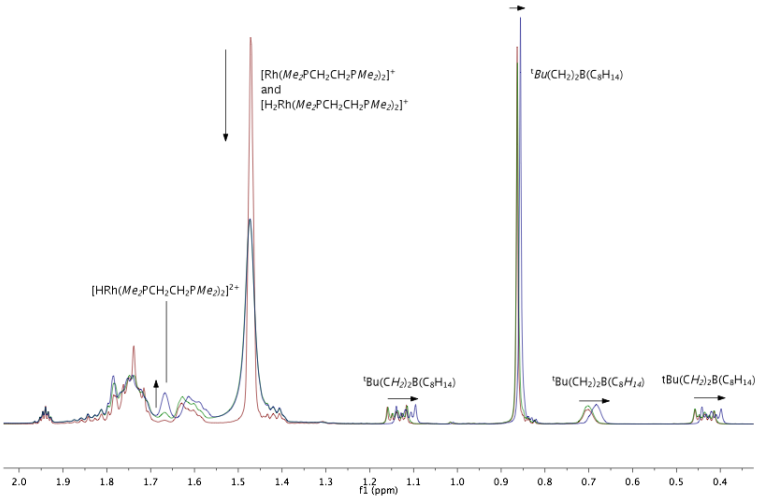

Figure 5.30. ^{1}H NMR time course (aliphatic region) of reaction of $[Rh(dmpe)_2]^+$ with ^{t}Bu$(CH_2)_2$B(C_8H_{14}), CO_2 and H_2. Red: before H_2/CO_2 addition. green, 1.5 hrs after H_2/CO_2 addition. yellow, 18 hrs after H_2/CO_2 addition.

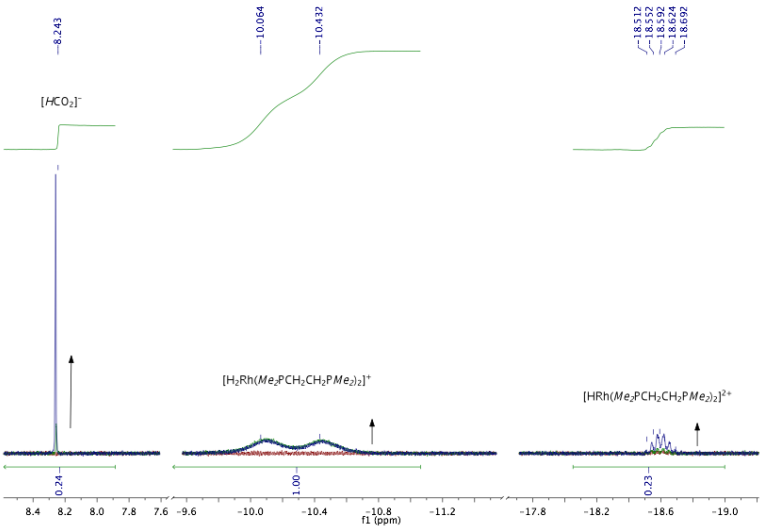

Figure 5.31. ^{1}H NMR time course (formate and hydride regions) of reaction of $[Rh(dmpe)_2]^+$ with ^{t}Bu$(CH_2)_2$B(C_8H_{14}), CO_2 and H_2. Red: before H_2/CO_2 addition. green, 1.5 hrs after H_2/CO_2 addition. yellow, 18 hrs after H_2/CO_2 addition.

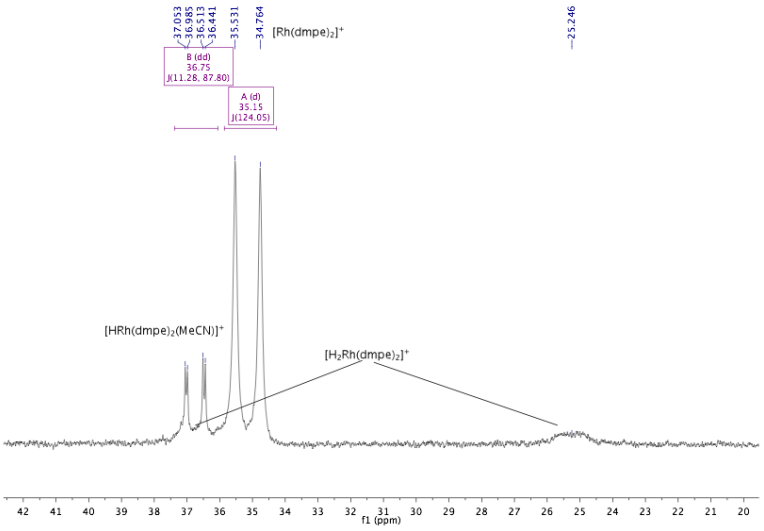

Figure 5.32. ^{31}P NMR (partially decoupled) 18 hours after reaction of $[Rh(dmpe)_2]^+$ with ^{t}Bu$(CH_2)_2$B(C_8H_{14}), CO_2 and H_2.

Attempted catalytic reactions

Acetonitrile. A J-Young NMR tube was charged with 5.0 mg (0.0102 mmol, 1 equiv) $[Ni(dmpe)_2][BF_4]_2$, 7.1 μL (0.0511 mmol, 5 equiv) NEt_3, 10.5 mg (0.0511 mmol, 5 equiv)

^{t}Bu(CH$_2$)$_2$B(C$_8$H$_{14}$), and ~0.6 mL CD$_3$CN. The tube was subjected to two freeze–pump–thaw cycles, and 1 atm of a 1:1 H_2:CO_2 mixture (mixed in a large round bulb on a vacuum line) was admitted. The reaction was monitored by NMR spectroscopy, and a small formate peak gradually grew in over 3 days, along with another product, δ ~6.8. Heating the tube to 60 °C for ~24 hours generated visible amounts of [HNi(dmpe)$_2$]$^+$, but also several unidentified products.

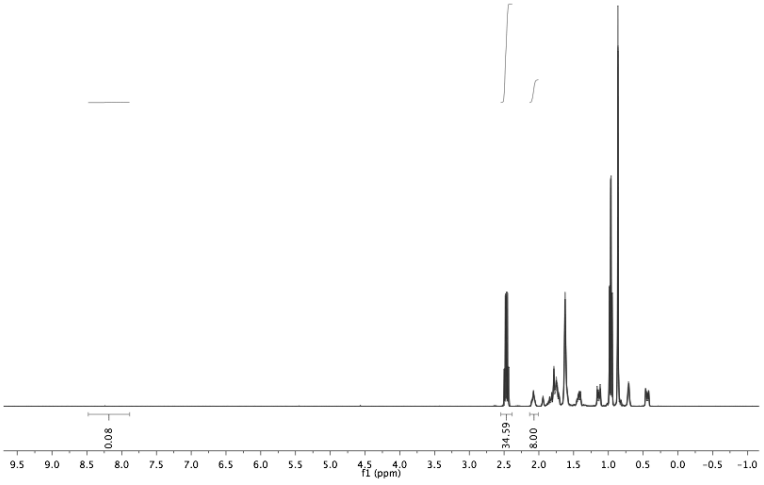

Figure 5.33. ^{1}H NMR time course of attempted catalysis in CD$_3$CN.

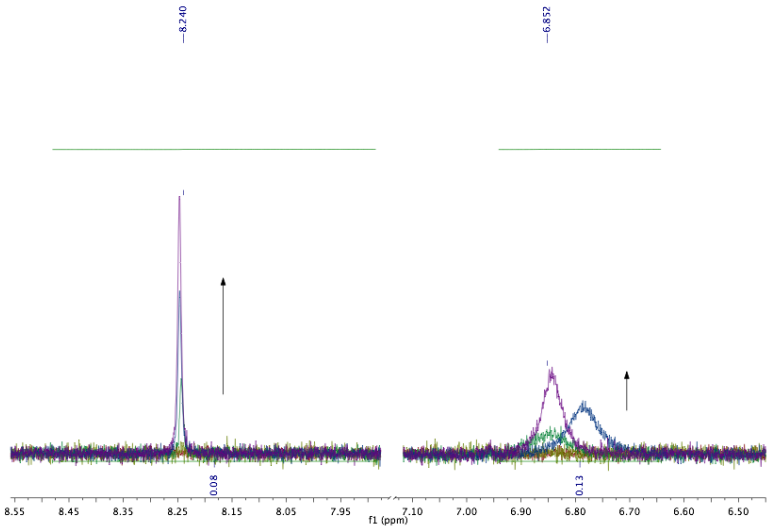

Figure 5.34. ^{1}H NMR time course (over 3 days) of attempted catalysis in CD_3CN.

Chlorobenzene. A J-Young NMR tube was charged with 35.5 mg (0.0174 mmol, 1 equiv) $[Ni(dmpe)_2][BAr^F{}_4]_2$, 10.0 μL (0.0695 mmol, 4 equiv) NEt_3, 3.6 mg (0.0174, 1 equiv) ^{t}Bu$(CH_2)_2$B(C_8H_{14}), and ~0.6 mL C_6D_5Cl. The Ni dication formed a yellow oil at the bottom of the tube if it was allowed to settle. The tube was subjected to two freeze–pump–thaw cycles, and 1 atm of a 1:1 mixture of H_2:CO_2 (mixed in a large round bulb on a vacuum line) was admitted to the tube. NMR spectroscopic monitoring showed steady generation of $[HNi(dmpe)_2][BAr^F{}_4]$, but no evidence of formate was observed. The $BAr^F{}_4$ signal grows in as the mostly insoluble oil $[Ni(dmpe)_2][BAr^F{}_4]_2$ reacts.

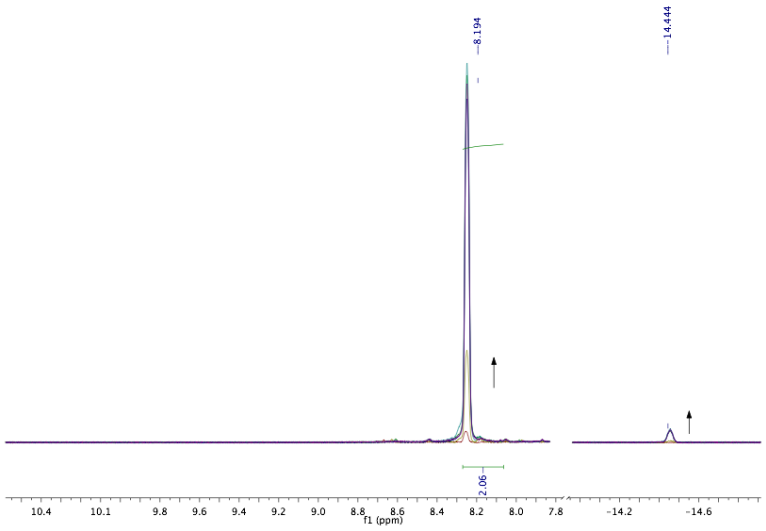

Figure 5.35. ^{1}H NMR time course of attempted catalysis in C_6D_5Cl.

Hydrogen cleavage reactions

Acetonitrile. A J-Young NMR tube was charged with 32.6 mg (0.0159 mmol) $[Ni(dmpe)_2][BAr^F{}_4]_2$, 8.9 μL (0.0639 mmol, 4 equiv) NEt_3, and ~0.6 mL CD_3CN. The tube was subjected to two freeze–pump–thaw cycles and 1 atm of H_2 was admitted. The reaction was monitored, revealing about 30% conversion to $[HNi(dmpe)_2]^+$ over 3 days.

Chlorobenzene. A J-Young NMR tube was charged with 29.0 mg (0.0140 mmol) $[Ni(dmpe)_2][BAr^F{}_4]_2$, 7.9 μL (0.0568 mmol, 4 equiv) NEt_3, and ~0.6 mL C_6D_5Cl. The Ni dication was insoluble, and formed an oil at the bottom of the tube. Initial NMR measurements detected no Ni species. The tube was subjected to two freeze–pump–thaw cycles and 1 atm H_2 was admitted. The tube was sealed and monitored by NMR, which revealed relatively rapid growth of $[HNi(dmpe)_2][BAr^F{}_4]$. After 18 hours, no insolubles were visible, and a large amount of Ni hydride was present. The two phase reaction prevented precise yields or equilibrium measurements.

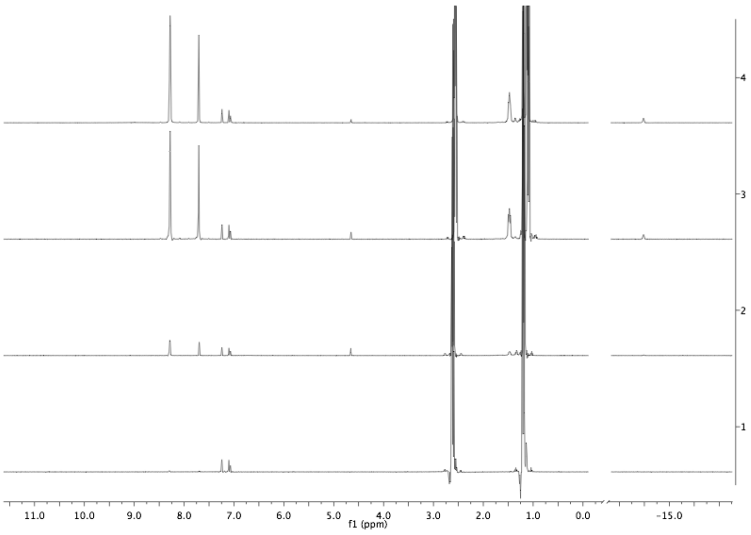

Figure 5.36. ^{1}H NMR time course of H_2 cleavage by $[Ni(dmpe)_2][BAr^F{}_4]_2$ (excess NEt_3 cut off).

References

1. (a) Benson, E. E.; Kubiak, C. P.; Sathrum, A. J.; Smieja, J. M. *Chem. Soc. Rev.* **2009**, *38*, 89; (b) Leitner, W. *Angew. Chem. Int. Edit.* **1995**, *34*, 2207.
2. (a) Saveant, J.-M. *Chem. Rev.* **2008**, *108*, 2348; (b) Hammouche, M.; Lexa, D.; Momenteau, M.; Saveant, J. M. *J. Am. Chem. Soc.* **1991**, *113*, 8455; (c) Bhugun, I.; Lexa, D.; Saveant, J.-M. *J. Am. Chem. Soc.* **1994**, *116*, 5015; (d) Bhugun, I.; Lexa, D.; Saveant, J.-M. *J. Am. Chem. Soc.* **1996**, *118*, 1769; (e) Bhugun, I.; Lexa, D.; Saveant, J.-M. *J. Phys. Chem.* **1996**, *100*, 19981; (f) Gennaro, A.; Isse, A. A.; Severin, M.-G.; Vianello, E.; Bhugun, I.; Saveant, J.-M. *J. Chem. Soc., Faraday Trans.* **1996**, *92*, 3963; (g) Wong, K.-Y.; Chung, W.-H.; Lau, C.-P. *J. Electroanal. Chem.* **1998**, *453*, 161.
3. (a) Dubois, M. R.; Dubois, D. L. *Acc. Chem. Res.* **2009**, *42*, 1974; (b) Steffey, B. D.; Curtis, C. J.; DuBois, D. L. *Organometallics* **1995**, *14*, 4937; (c) Jeoung, J.-H.; Dobbek, H. *Science* **2007**, *318*, 1461.
4. Boffa, A.; Lin, C.; Bell, A. T.; Somorjai, G. A. *J. Catal.* **1994**, *149*, 149.
5. Laitar, D. S.; Muller, P.; Sadighi, J. P. *J. Am. Chem. Soc.* **2005**, *127*, 17196.
6. Chakraborty, S.; Zhang, J.; Krause, J. A.; Guan, H. R. *J. Am. Chem. Soc.* **2010**, *132*, 8872.
7. Stephan, D. W.; Erker, G. *Angew. Chem. Int. Ed.* **2010**, *49*, 46.
8. Ashley, A. E.; Thompson, A. L.; O'Hare, D. *Angew. Chem. Int. Edit.* **2009**, *48*, 9839.

9. Rozovskii, A. Y.; Lin, G. I. *Top. Catal.* **2003**, *22*, 137.
10. (a) Miller, A. J. M.; Labinger, J. A.; Bercaw, J. E. *J. Am. Chem. Soc.* **2008**, *130*, 11874; (b) Elowe, P. R.; West, N. M.; Labinger, J. A.; Bercaw, J. E. *Organometallics* **2009**, *28*, 6218; (c) Miller, A. J. M.; Labinger, J. A.; Bercaw, J. E. *J. Am. Chem. Soc.* **2010**, *132*, 3301; (d) Miller, A. J. M.; Labinger, J. A.; Bercaw, J. E. *Organometallics* **2010**, *29*, 4499; (e) West, N. M.; Miller, A., J. M.; Labinger, J. A.; Bercaw, J. E. *Coord. Chem. Rev.* **2010**, *In Press*.
11. Miedaner, A.; DuBois, D. L.; Curtis, C. J.; Haltiwanger, R. C. *Organometallics* **1993**, *12*, 299.
12. (a) Berning, D. E.; Noll, B. C.; DuBois, D. L. *J. Am. Chem. Soc.* **1999**, *121*, 11432; (b) Berning, D. E.; Miedaner, A.; Curtis, C. J.; Noll, B. C.; Rakowski DuBois, M. C.; DuBois, D. L. *Organometallics* **2001**, *20*, 1832; (c) Ciancanelli, R.; Noll, B. C.; DuBois, D. L.; DuBois, M. R. *J. Am. Chem. Soc.* **2002**, *124*, 2984; (d) Curtis, C. J.; Miedaner, A.; Ellis, W. W.; DuBois, D. L. *J. Am. Chem. Soc.* **2002**, *124*, 1918; (e) Price, A. J.; Ciancanelli, R.; Noll, B. C.; Curtis, C. J.; DuBois, D. L.; DuBois, M. R. *Organometallics* **2002**, *21*, 4833; (f) Miedaner, A.; Raebiger, J. W.; Curtis, C. J.; Miller, S. M.; DuBois, D. L. *Organometallics* **2004**, *23*, 2670; (g) Raebiger, J. W.; DuBois, D. L. *Organometallics* **2005**, *24*, 110; (h) DuBois, D. L.; Blake, D. M.; Miedaner, A.; Curtis, C. J.; DuBois, M. R.; Franz, J. A.; Linehan, J. C. *Organometallics* **2006**, *25*, 4414; (i) Nimlos, M. R.; Chang, C. H.; Curtis, C. J.; Miedaner, A.; Pilath, H. M.; DuBois, D. L. *Organometallics* **2008**, *27*, 2715.
13. DuBois, D. L.; Berning, D. E. *Appl. Organomet. Chem.* **2000**, *14*, 860.
14. Wilson, A. D.; Miller, A. J. M.; DuBois, D. L.; Labinger, J. A.; Bercaw, J. E. *Inorg. Chem.* **2010**, *49*, 3918.
15. Kaljurand, I.; Kutt, A.; Soovali, L.; Rodima, T.; Maemets, V.; Leito, I.; Koppel, I. A. *J. Org. Chem.* **2005**, *70*, 1019.
16. Pangborn, A. B.; Giardello, M. A.; Grubbs, R. H.; Rosen, R. K.; Timmers, F. J. *Organometallics* **1996**, *15*, 1518.
17. Hirano, K.; Yorimitsu, H.; Oshima, K. *Org. Lett.* **2005**, *7*, 4689.
18. Silavwe, N. D.; Goldman, A. S.; Ritter, R.; Tyler, D. R. *Inorg. Chem.* **1989**, *28*, 1231.